SPACE EXPERIMENTS

The study of cosmic rays (CR) can be described as a two step process :

– understanding and calibrating nature's beam by more measurements of CR composition and spectra, better theory (CR origin and acceleration) and better simulation tools

– search for new physics
Discovery potential is very promising : search for nuclear antimatter or for strange states of matter, indirect search of dark matter using $\bar{p}$, $\bar{d}$, e^+ and γ rays, ultra heavy particle searches using CR having Extreme Energies.

OUTLINE

– **Spacial environment**
– **Cosmic Rays spectrum**
– **Balloon experiments**
– **Satellite experiments**

The Solar Wind

The solar wind is the supersonic flow of plasma produced in the upper reaches of the solar atmosphere. Supersonic means that the flow velocity of the solar wind is large compared to the average thermal velocity of the ions.

The solar wind was hypothesized to exist on the basis of a number of pre-space age observations, including observations of comets ; it was discovered by Biermann in 1951.

Some of its characterics are :
– plasma of electrons and ions moving radially outward from the sun
– speed $\sim 300 - 500$ km/s near Earth orbit
– needs ~ 4 days to reach Earth
– Density ~ 10 ions/cm^3 at the Earth orbit
– fills the entire solar system and interacts with magnetic field planets creating magnetospheric cavities (Mercury, Earth, Jupiter, Saturn, Uranus and Neptun).

The Earth magnetic Field

Over 4 to 5 Earth radius (R_E = 6378 km), the magnetic field is well approximated with a dipole field with magnetic moment $M = 8.1 \times 10^{22}$A.m^2.

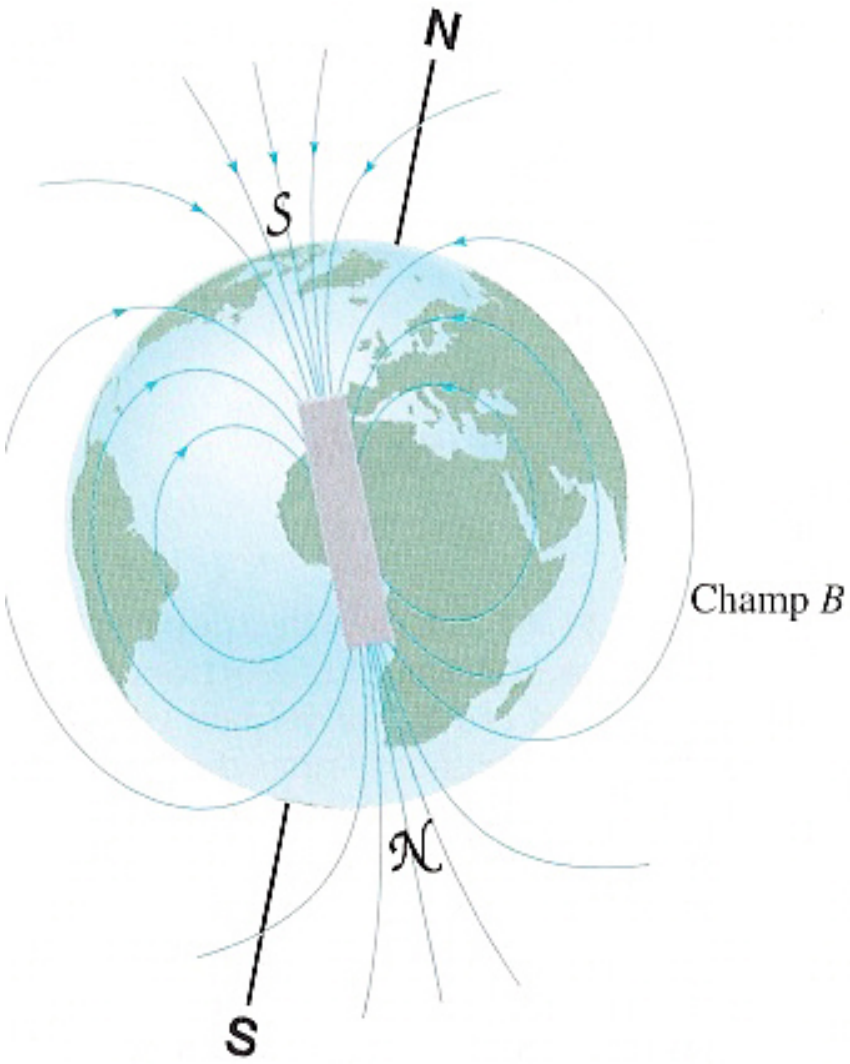

- The geomagnetic and geographic poles do not coincide. In May 2003, in geographic coordinates :
  North magnetic pole : $82^o N, 83^o W$
  South magnetic pole : $74^o S, 127^o E$.
- The North pole is in fact the south geomagnetic pole.
- The closest dipole is displaced from the Earth center by 436 km in direction of the Pacific North-west, and its axis is inclined by 11° with respect to the Earth spin axis.
- The magnetic field changes with time : it has reversed itself some 300 times in the past 170 million years and may have done so just 30000 years ago.

The Earth magnetic Field

In spherical coordinates (r, λ, ϕ) in the geomagnetic referential, the magnitude and direction of the geomagnetic field vector at any point on the surface and at points above the surface out of a few Earth radii are obtained within an accuracy of 10% using the following formulae (2% with off-center dipole) :

$$B_r = -\frac{\mu_o}{4\pi}\frac{2M sin\lambda}{r^3}, B_\lambda = \frac{\mu_o}{4\pi}\frac{M cos\lambda}{r^3}, B_\phi = 0$$

The magnitude of $\vec{B}$:

$$B = \frac{\mu_o}{4\pi}\frac{M}{r^3}\sqrt{1+3sin^2\lambda} \sim \frac{1}{r^3}$$

$B_{eq} = 3.134\ 10^{-5}$ T at the equator and double value at the Pole.

The equation of a field line is given by :

$$r = r_o cos^2\lambda = L\ R_E \cos^2\lambda$$

where L is defined, for a given field line, as the distance to the center of Earth from the point where the field line crosses the magnetic equator, in unit of Earth radius.

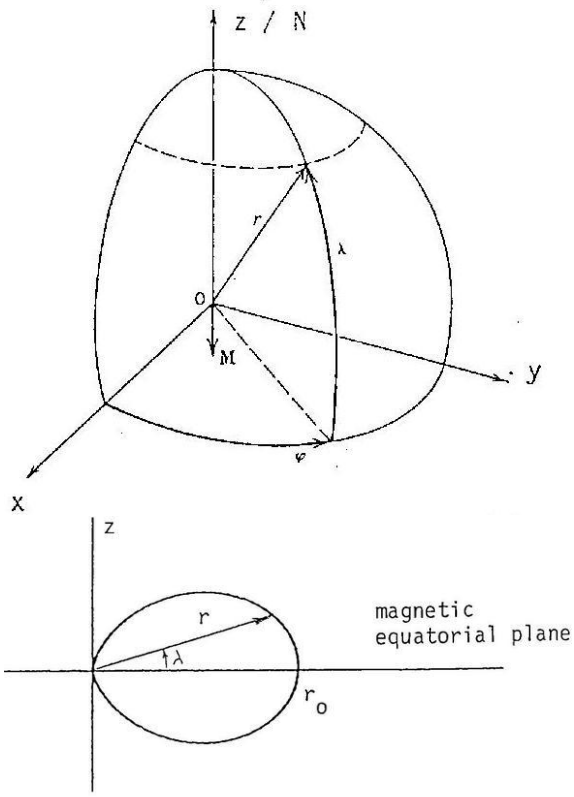

The Earth magnetic Field

In a pure centered dipole field, isointensity lines would be horizontal. Contours are in Gauss.

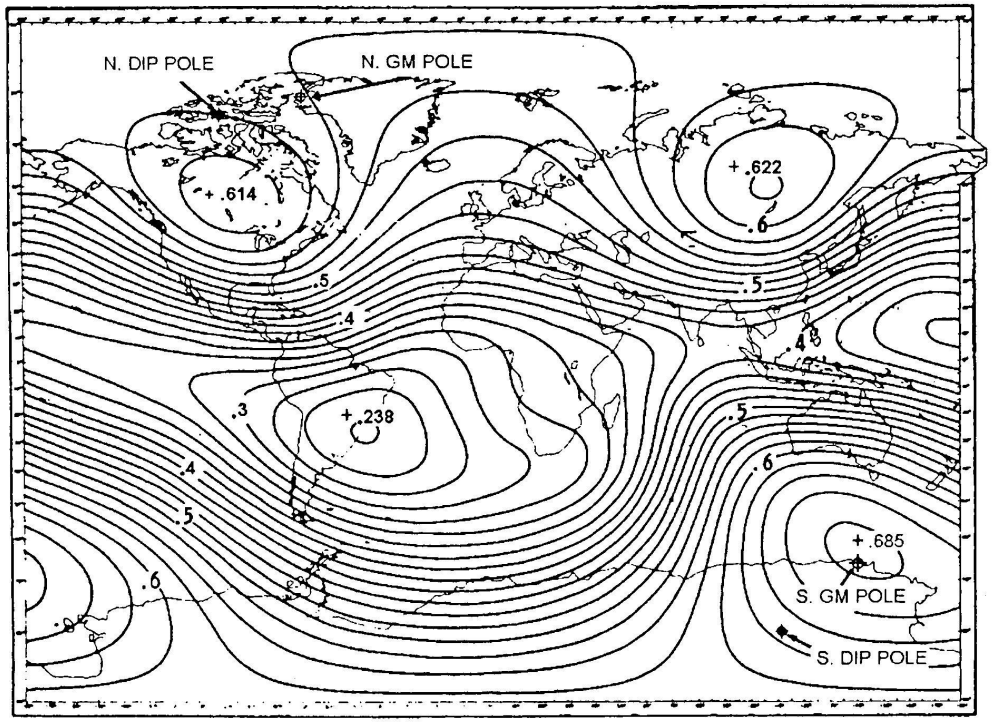

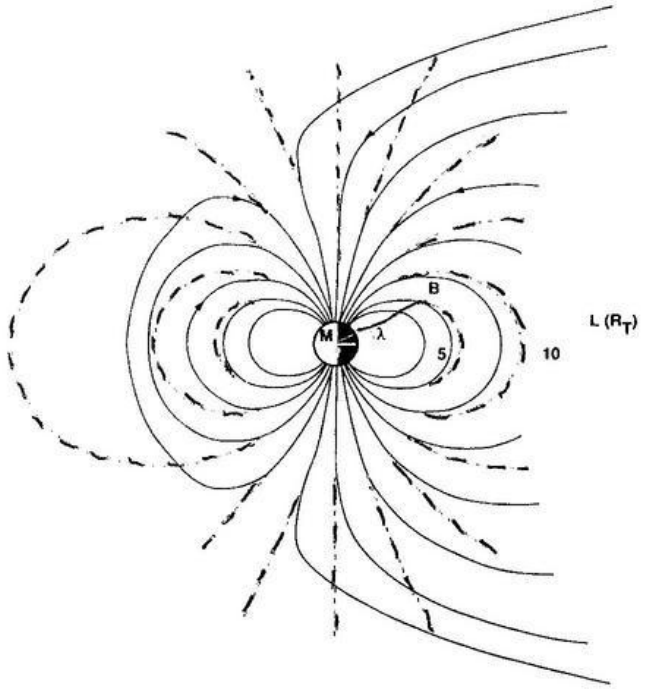

The Magnetosphere

In the absence of an interplanetary plasma, the earth's dipole field would extend indefinitely in all directions. However, the geomagnetic field produces a semipermeable obstacle to the solar wind and the resulting interaction produces a cavity, the *magnetosphere*, around which most of the plasma flows.

The moving plasma compresses the field on the sunward side, flows around the magnetic barrier, and distends the field lines into a tail extending several million kilometers down-wind from the Earth.

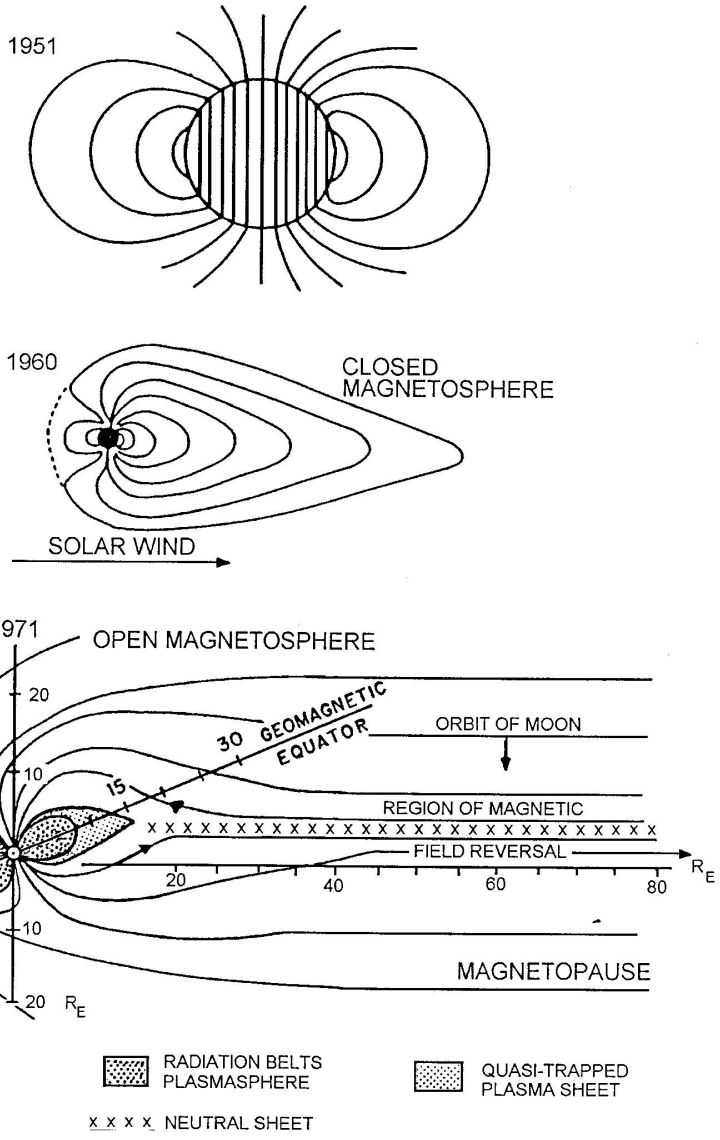

The Magnetosphere

– **Bow shock** : where the initial decceleration and deflection of solar wind occurs. Its thickness is $\sim$ 50-100 km
– **Magnetopause** : the boundary between the region dominated by the geomagnetic field on one side and the region dominated by the solar wind plasma pressure on the other side. By equating the total pressure on one side to the total pressure on the side, one can righly estimate the location of this boundary as ~ 9 Earth radius which is in agreement with the observations.

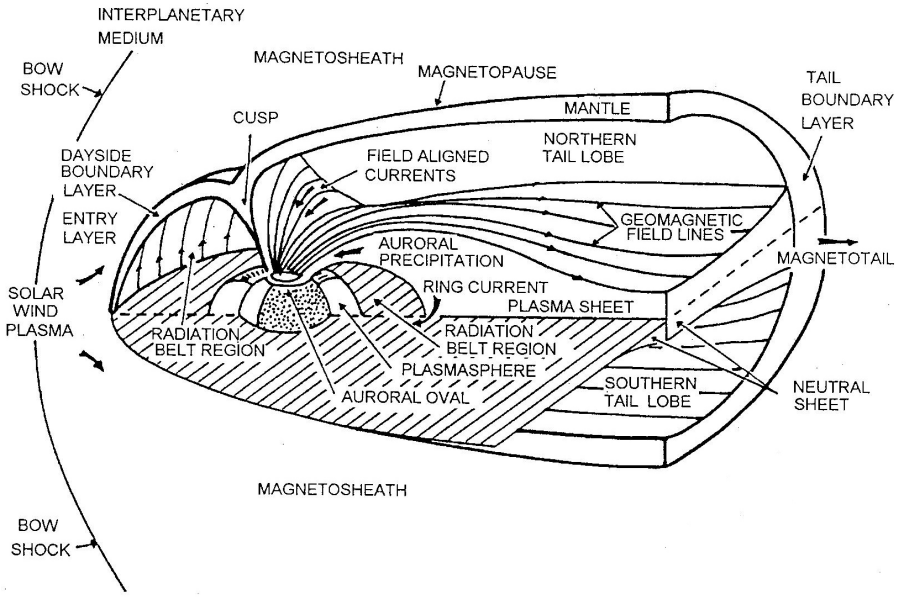

– **Magnetosheath** : between the bow shock and the magnetopause. It is filled with plasma coming directly from the solar wind.
– **Polar Cusps** : 2 singularities regions where the field lines disappear and particles/plasma can penetrate into the magnetosphere, even to the atmosphere giving borealis aurora.
– **Radiation belts** : well inside the magnetosphere.

Radiation Belts

In general trapping requires stable magnetic fields. But

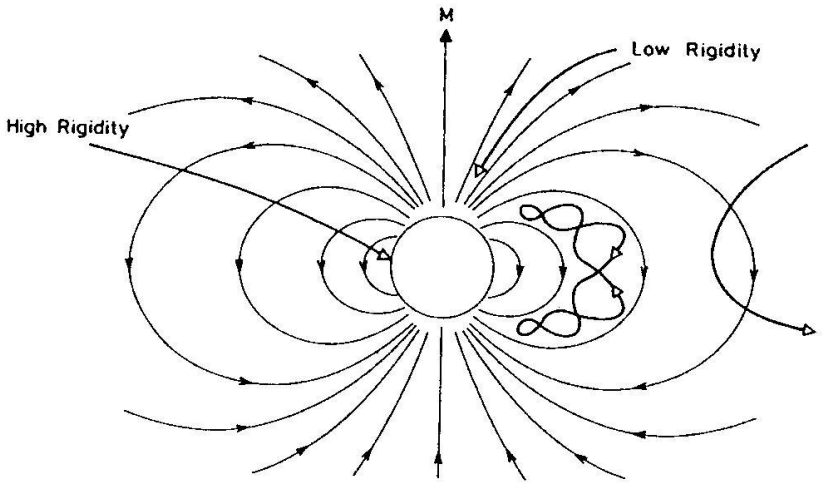

Radiations belts are toroidal structures well inside the magnetosphere.

– On the high altitude side : magnetic field fluctuations induced by solar wind variability prevent long term trapping.
– On the low altitude side : the atmosphere limits the radiation belts particles to regions above 200-1000 km because collisions between trapped particles and atmosphere constituents slow down the trapped particules or deflect them into the denser atmosphere.

Thus, the region of prime interest is the volume of stable magnetic field between $\sim 200km$ and $7R_E$ at the equator.

The radiation belts are of primary concern for the satellite designer because of the effects of penetrating radiation on electronics.

Radiation Belts

The motion of a charged particle in a static magnetic dipole field may be regarded as the superposition of 3 different quasi-periodic motions :

– a circular motion in a plane perpendicular to the local magnetic field referred as **gyration**

– a much slower North-South oscillation between 2 mirror points along a magnetic field line referred as **bouncing**.

– a still-much slower rotation of the guiding line around the polar axis referred as **drifting**

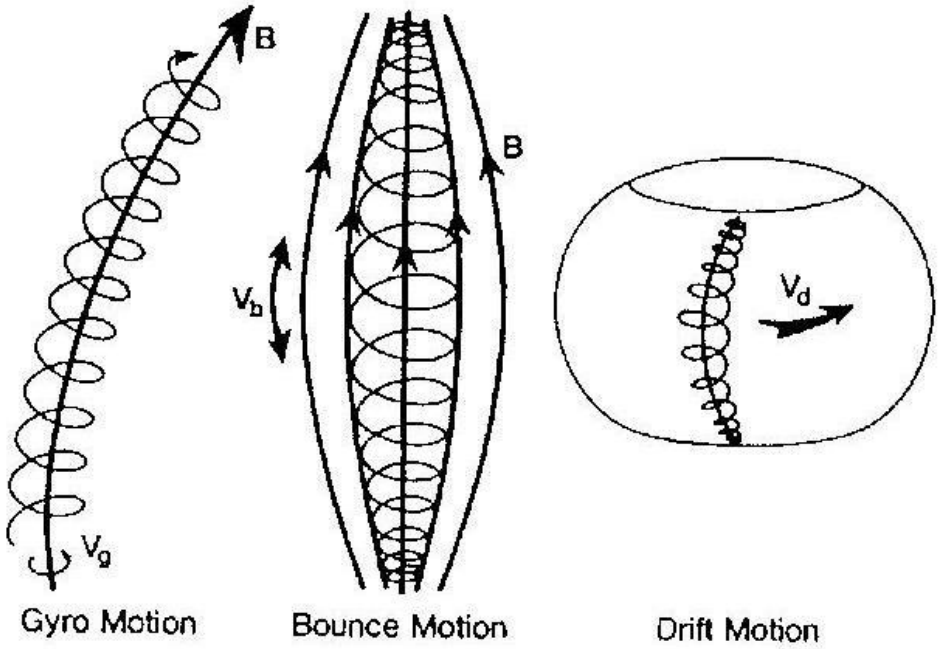

Gyration in a uniform magnetic field

In a uniform magnetic field ($\vec{B}$), a charged particle (q) describes a helix, a circular motion in the plane perpendicular to $\vec{B}$ being superimposed on a uniform motion parallel to $\vec{B}$. The pitch angle of the helix is the angle between the particle velocity and the magnetic field given by $\alpha = \tan^{-1}(v_\perp / v_\parallel)$:

$$\rho = \frac{p_\perp}{Bq} = \frac{\gamma m v_\perp}{Bq} \qquad \omega_g = 2\pi \frac{v_\perp}{2\pi\rho} = \frac{Bq}{\gamma m} \qquad \tau_g = \frac{2\pi}{\omega_g}$$

Calculing ρ gives values much smaller than R_E even for high energy particles and the magnetic filed does not vary much over a gyration. Nevertheless, the slight deviations from helical motion which are produced by ΔB accumulate over time and lead to important perturbations.

To study the dynamic of charged particle in a magnetic field changing slightly, one uses **adiabatic invariants**.(A system can change from one state of motion to another and keep the same integral of action). In particular one can show that the quantity $J_1 = \pi p_\perp^2 / (ZB)$ is constant over a gyration motion. In the non-relativistic case, J_1 is proportional to the magnetic moment of an orbiting charged particle $\mu = p_\perp^2 / (2mB)$.

$$J_1 = \pi \frac{p_\perp^2}{ZB} \sim \frac{p^2 sin^2 \alpha}{B}$$

Gyration in a slowly varying magnetic field

As the quantity J_1 must be constant, when a particle penetrates into regions of larger magnetic field (pole), the pitch angle (α) must increase.
When $\alpha = 90°$, the longitudinal motion stops and is then reversed. A similar situation happens when the particle approaching the other pole. The particle is then bounced back and forth in between 2 mirror points.

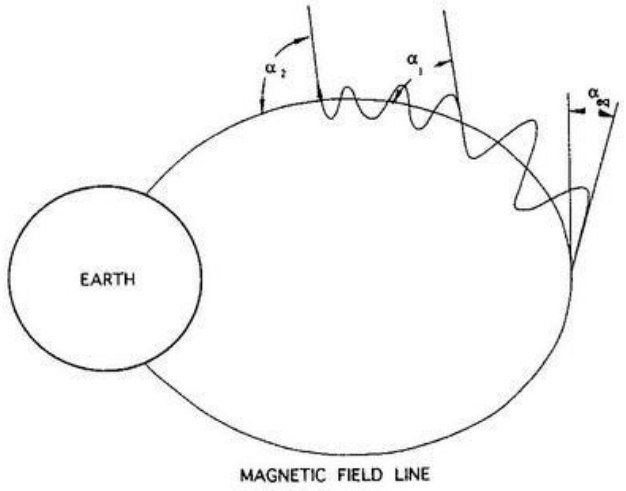

If the pitch angle is 90° at the point where the magnetic field is B_M, then

$$J_1 \sim \frac{\sin^2 \alpha}{B} = \frac{\sin^2(90°)}{B_M}$$

$$\rightarrow \quad \sin^2(\alpha) = \frac{B}{B_M}$$

One can calculate the bouncing period,τ_b :

$$\tau_b = 6.37 \times 10^6 \, L \, g(\lambda_m) v^{-1} [\text{s}]$$

where $g(\lambda_m)$ is a geometrical quantity depending on the mirroring latitude

Ceintures de radiation

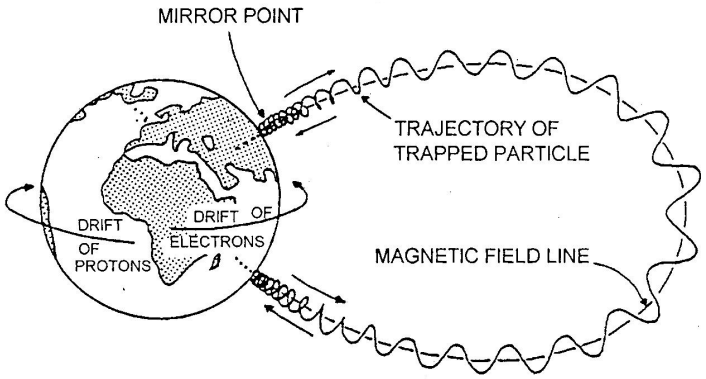

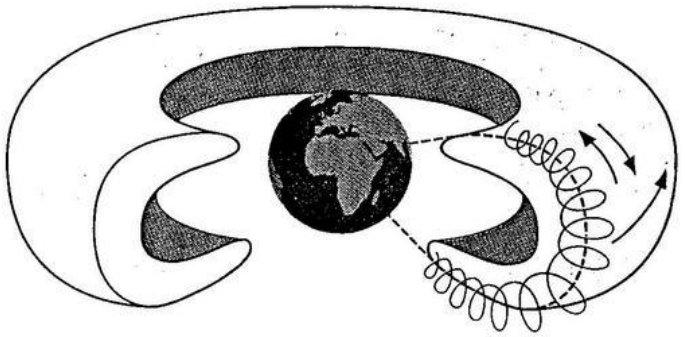

	Gyration radius ρ [km]	Gyration period τ_g [10^{-3}s]	Bouncing period τ_b [s]	Drifting period τ_d [mn]
p 10 MeV Low altitude :$L = 1.5R_E$	49	7	0.65	3
p 10 MeV High altitude :$L = 4R_E$	932	130	1.7	1.1
e^- 1 MeV Low altitude :$L = 1.5R_E$	0.5	11.33 $\times 10^{-3}$	0.1	44
e^- 1 MeV High altitude :$L = 4R_E$	10	0.2	0.3	16

for equatorially trapped particles.

Van Allen Radiation Belts

It is customary to describe the radiation belts as consisting of 2 zones :
1) an external one for $L > 2.5$, consisting of e^- fed by an injection mecanism from the magnetospheric tail
2) an inner one for reions inside $L \sim 2.5$ containing both e^- and p and fed mainly by β desintegration of free neutrons $n \longrightarrow p^+ + e^- + \bar{\nu}_e$.

Protons

Single maximum distribution
Energies extend up to several hundred MeV, making the proton flux the most penetrating of all trapped particles.
Maximum flux on the equatorial plane at about $L = 3.1$.
The intensity contours become more closely spaced below $L = 1.5$ where the Earth's atmosphere becomes dense enough to remove energetic protons.

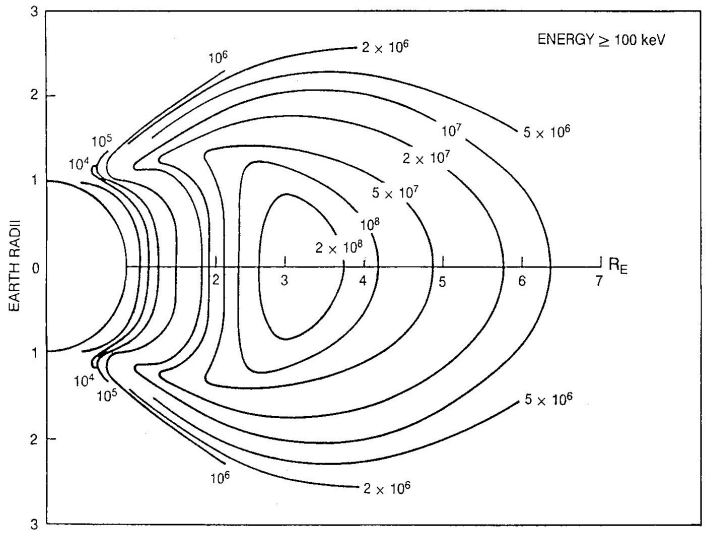

Omnidirectional fluxes in $cm^{-2}s^{-1}$.

Van Allen Radiation Belts

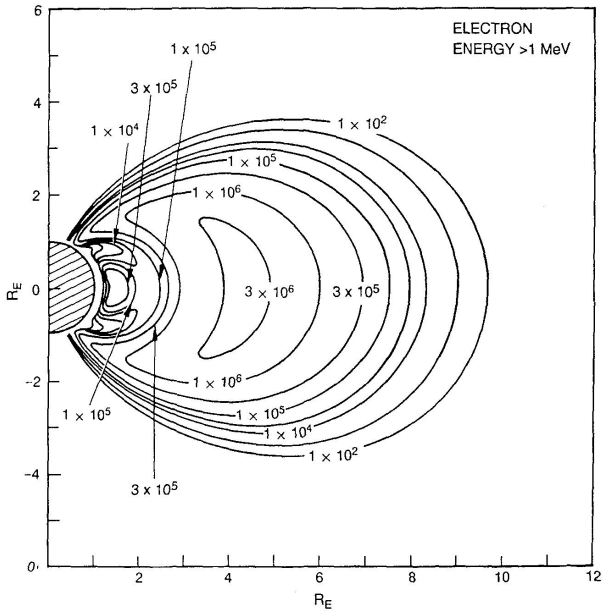

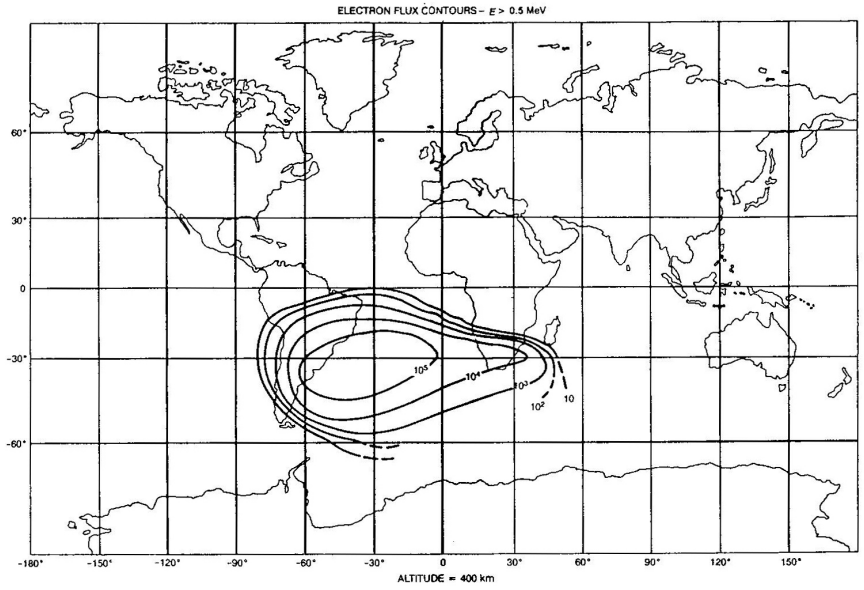

Electrons

– Occur throughout the Earth's trapping regions

– Energies up to several MeV.

– At $L = 3 - 5$, high energy electrons are most penetrating, most damaging.

– Rapide decrease in flux with increasing energy and a minimum at $L = 2.5$

At low altitude, assymmetries in the geomagnetic field distort the contours of radiation intensity, in particular in SAA. In order to mirror at a constant B value, particules must descend to lower altitudes while drifting. Thus, for given altitude, the radiation intensity is much higher over the SAA than elsewhere.

Geomagnetic cut-off

As charged particles are deviated by magnetic fields, not all particules have the possibility to reach the Earth. There is a geomagnetic cut-off. It is usually defined in terms of the magnetic rigidity, $R = pc/Ze$ where p is the momentum and Z the charge. An ion will be able to reach a point M only if its rigidity is larger than a rigidity cut, R_c.

At a point M defined by its distance to the Earth center (r) and its latitude (λ), an ion with velocity vector at an angle ϕ with respect to the meridien plane :

$$R_c[GV] = 14,9(\frac{R_E}{r})^2 \frac{4cos^4\lambda}{(1+\sqrt{1-cos^3\lambda cos\phi})^2}$$

So, for a particle arriving vertically ($\phi = \pi/2$), one simply has :

$$R_c = 14,9(\frac{R_E}{r})^2 cos^4\lambda$$

$\longrightarrow$ rigidity cut affects mainly low latitudes and even drops to zero at magnetic poles.

Particles can reach the Earth only if $p \geq 14.9Ze\ cos^4\lambda\ [GeV/c]$

Z =1	$\lambda = 0^o$	$p \geq 14.9\ GeV/c$
	$\lambda = 40^o$	$p \geq 5.3\ GeV/c$
	$\lambda = 60^o$	$p \geq 0.93\ GeV/c$

Cosmic Rays History

Cosmic radiation (CR) discovered in 1912 by V.F.Hess in balloon flights.

– In the early days, CR meant a study of the basic properties of electricity and magnetism

– Later, CR was particle physics until the large accelerators were built.

Particle	Year	Discoverer (Nobel Prize)	Method
e^-	1897	J.J. Thomson (1906)	Discharges in gases
p	1919	E. Rutherford	Natural radioactivity
n	1932	J. Chadwik (1935)	Natural radioactivity
e^+	1933	C.D. Anderson (1936)	Cosmic Rays
$\mu^\pm$	1937	S. Neddermeyer	Cosmic Rays
$\pi^\pm$	1947	C.F. Powell (1950)	Cosmic Rays
$K^\pm$	1949	C.F. Powell (1950)	Cosmic Rays
π^0	1949	R. Bjorklund	Accelerator
K^0	1951	R. Armenteros	Cosmic Rays
Λ^0	1951	R. Armenteros	Cosmic Rays
Δ	1952	C.D. Anderson	Cosmic Rays
Ξ^-	1952	R. Armenteros	Cosmic Rays
$\Sigma^\pm$	1953	A. Bonetti	Cosmic Rays
p^-	1955	O.Chamberlain (1959)	Accelerators
		E. Segre' (1959)	
anything else	>1955	various groups	Accelerators
ν oscillations	1998	SuperKamiokande	Cosmic Rays

Cosmic rays history

– Still later, it became astrophysics- studying the Galactic sources of the lower energy CR, the magnetic fields in the heliosphere and the Galaxy, and the acceleration mechanisms in supernovae shocks.
– Today, CR astrophysics touches on the nuclear astrophyscis of stars and supernovae, particle physics at energies above those achievable by accelerators, the cosmology of the microwave and IR backgrounds, the Galactic physics of chemical evolution and interstellar medium processes, and unexplored physics at extremely high energies.

The experimental technics are wide-ranging as well, with experiments that could be held in one hand and huge air-shower arrays covering thousands of square kilometers (AUGER).

Cosmic Rays : Total Spectrum

Energy : > 12 orders of magnitude, Intensity : > 30 orders of magnitude

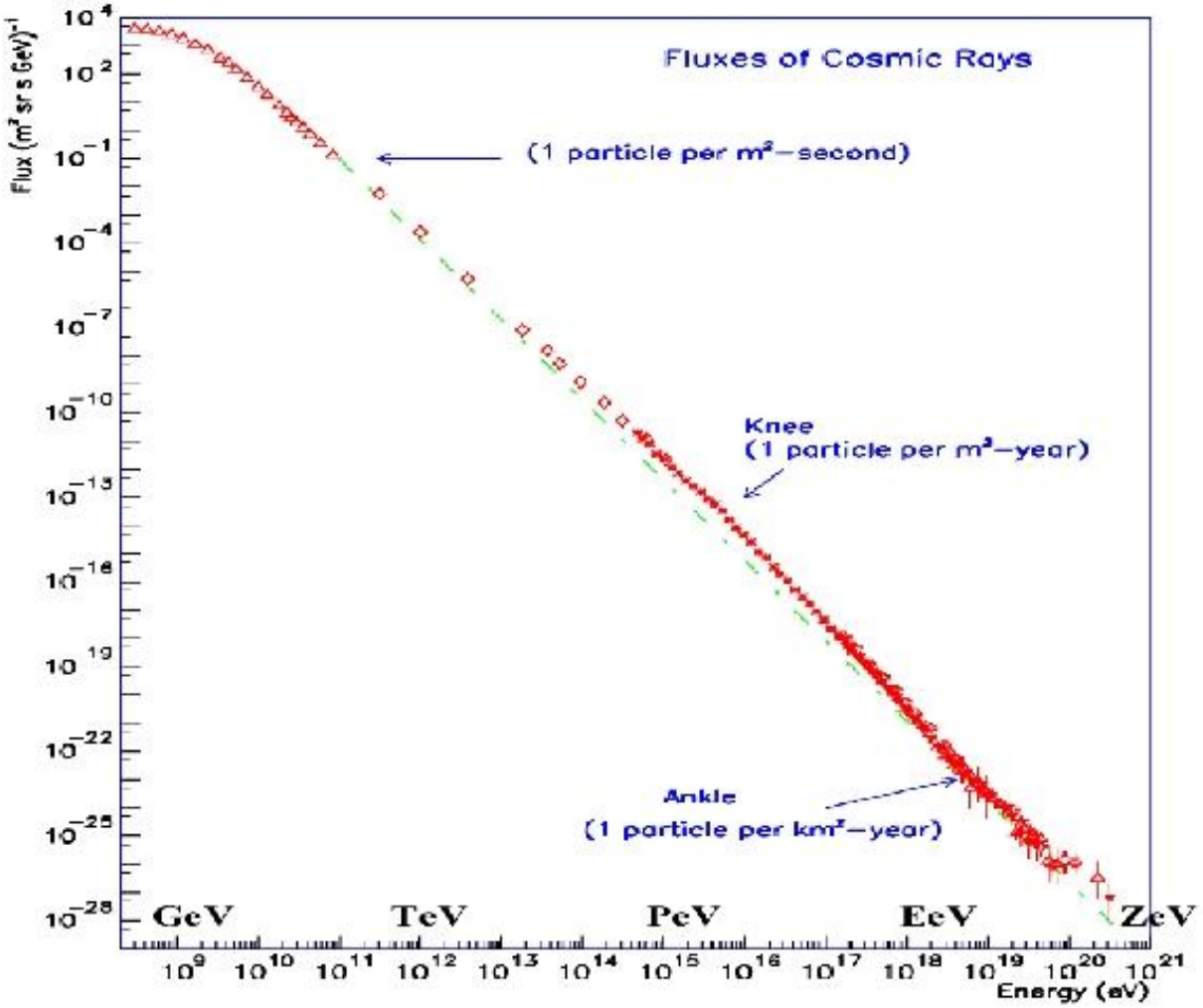

Origin of the *knee* not clear : Change in
– acceleration mechanism
– propagation mechanism
– elementary composition
– in interaction characteristics due to a new particle

Power law :
$\Phi \sim E^{-2.7} \rightarrow$*Knee*
$\Phi \sim E^{-3.0}$ from *knee* to *ankle*
$\Phi \sim E^{-2.8}$ above *ankle* ? ? ?

Cosmic Rays : Total Spectrum

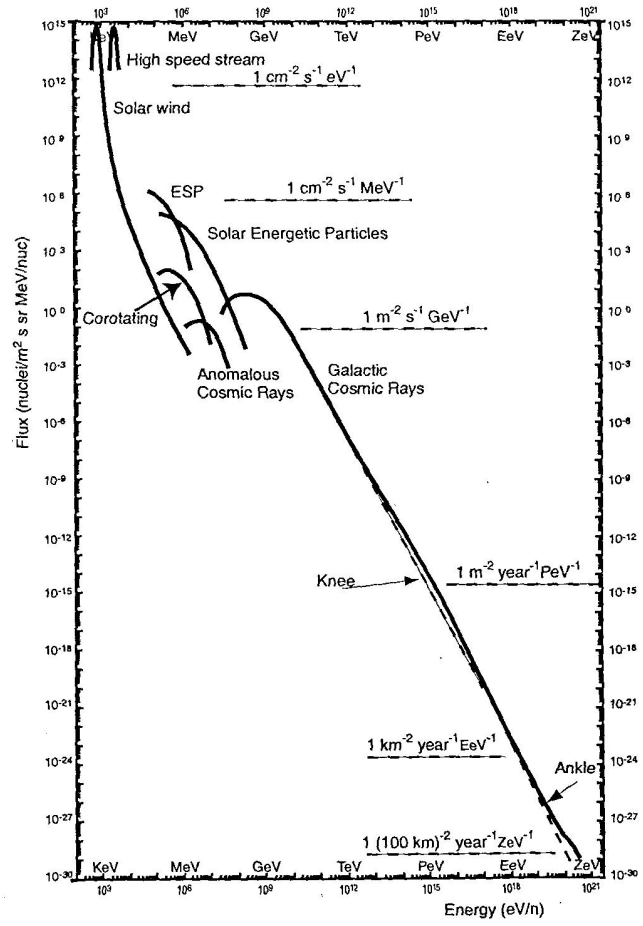

– **Solar Energetic Particles (SEP)** originating from solar eruptions : p few tenth MeV et anti-correlated with solar activity.
– **Anomalous Cosmics Rays (ACR)** coming from interstellar space outside the heliopause (low energy particles $\leq 100 MeV/n$, with Z=1) resulting from neutral particles penetrating the heliosphere, and being then ionized. Their composition differs from other CR ; more He than p and much more O_2 than C.
– **Galactic Cosmic Rays (GCR)**, the most abundant coming from outside solar system, but mainly from our galaxy. They are mostly produced and accelerated in supernovae explosions.

Below ~ 2 GeV, CR are affected by solar activity.

Cosmic Rays composition

p and He nuclei are the two dominant components ($p = 90\%$, $He \sim 9\%$)
All elements are present from hydrogen up to uranium.

The atoms reach the heliosphere fully ionized.

Measurements from RUNJOB/JACEE/ATIC up to 100 TeV

Absolute fluxes and spectrum shapes are fundamental information and indispensible for calculation of the accurate fluxes of atmospheric ν.

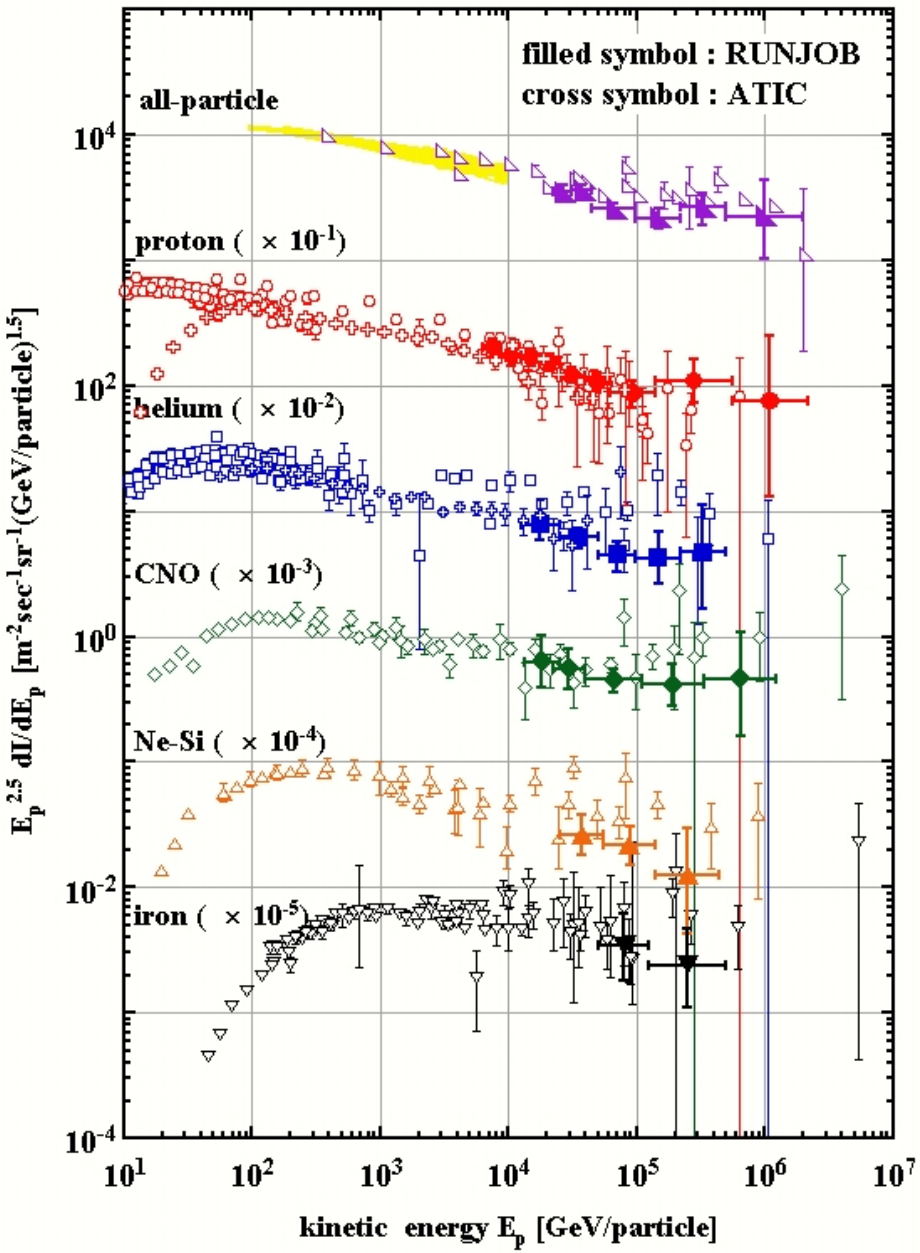

Cosmic Rays Composition

The chemical composition of GCR is very similar to the solar elemental abundances, with the exception :

– H, He enriched
– Li, Be, B enriched
– Sc, Ti, V, Cr, Mn enriched

The last 2 group elements not produced in the primordial nucleosynthesis (except ^{7}Li), nor made in stars

Li, Be and B are produced by spallation reactions involving p and α colliding with C,N,O nuclei in the supernova explosion. Similarily Sc, Ti, V, Cr, Mn are spallation from Fe. They are produced by collisions of cosmic rays in the interstellar medium (ISM).

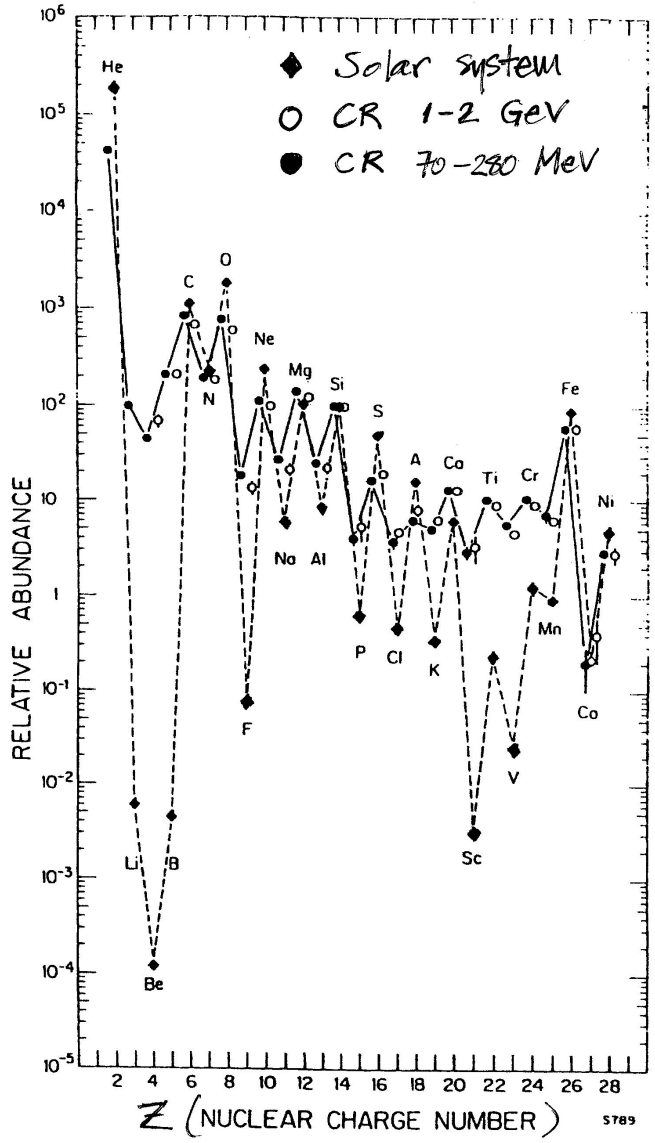

Cosmic Rays Propagation

From the knowledge of spallation cross sections, one can learn about the amount of matter traversed by CR between production and observation.

The mean amount of matter traversed is of the order of $X = 5$ to $10\ g\ cm^{-2}$. The density in the disk of galaxy is $\rho_N \sim 10^{-24} g\ cm^{-3} \sim 1\ proton/cm^3$, so this thickness of material corresponds to a distance of :

$$l = \frac{X}{\rho_N} \sim 5 \times 10^{24}\text{cm} \sim 1000\ \text{kpc}$$

$$t_c = \frac{l}{c} \sim 10^7\text{years.}$$

So as $l \gg d \sim 0.1$kpc, the half-thickness of the galaxy disk, this implies that CR confinement is a diffuse process in which the particles rattle around for a long time before escaping into intergalactic space. Another way is to measure the ^{10}Be isotope ; due to its long lifetime, the ^{10}Be isotope is used as a galactic chronometer for the measurement of the time of confinement of CR in the galaxy.

Experimental Constraints in space

– Number of particles above a given energy drops off sharply with increasing energy ⟶ long duration or/and large acceptance detector
– Accurate measurements of $\bar{p}$ spectrum requires a high rejection power against e^- as well as e^+ measurement requires a high rejection against p

– no man intervention
– Acceleration during start ($\sim$ 9g)and landing up to 20g for balloons
– Vibrations in a wide range of frequencies and amplitudes
– Temperature variations -180^o to +50^{o}C
– Weight limited
– Datarate 1 Mbyte/s via 1 datalink
– Power consumption limited

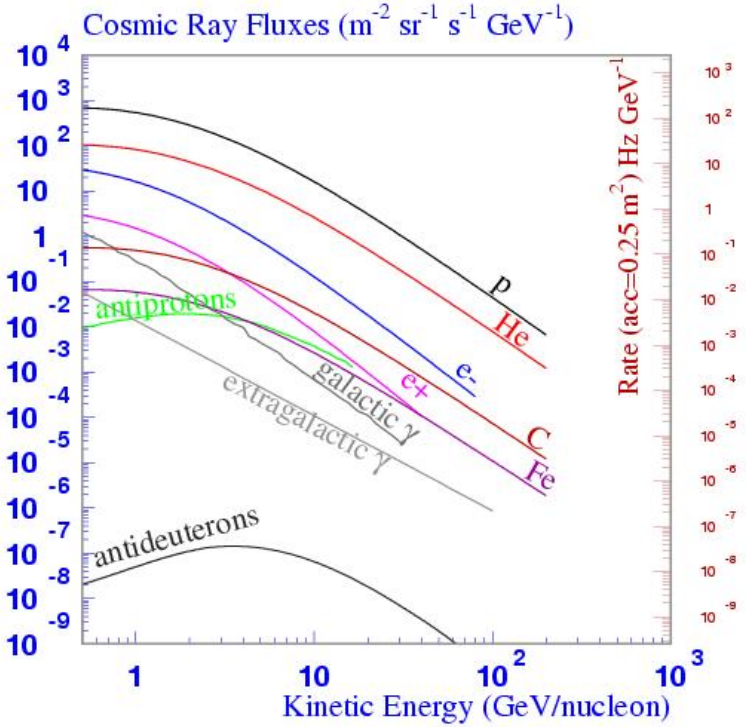

Balloon-born experiments

Experiment	Magnet	Flight location	Flight duration	Physics aims	Energy GeV/n
HEAT	Supra	NM+Canada	22 hrs	$e^-, e^+, \bar{p}$	4-30
CAPRICE	Supra	New Mexico	$\sim$20 hrs	$d, He, \bar{p}, e^+$	$3 \sim 100$
ISOMAX	Supra	Canada	$\sim$13 hrs	$3 < Z < 8$	< 4
TIGER	no	Antartica	31.8 days	$26 < Z < 40$	
ATIC	no	Antartica	19.7 days	$1 < Z < 28$	20- 10^5
RUNJOB	no	TransSiberia	6 days	$1 < Z < 28$	7- 10^6
JACEE	no	USA/Antartica	9-15 days	$1 < Z < 28$	$10^4 - 10^6$
BESS	Supra	Canada	20 hrs	$p, He, \bar{p}, \overline{He}, \bar{d}$	0.2-1.5
BESS-TeV	Supra	Canada	11.3 hrs	p, He	< 1000
BETS	no	Antartica	20-30 days	e^-	up to 500
BESS-Polar	supra	Antartica		$\bar{p}, \bar{d}, \bar{He}$	0.1 -4
CREAM	no	anywhere	100 days	$1 < Z < 28$	$10^3 - 10^5$

geomagnetic cut-off in Canada : 0.4 GV

geomagnetic cut-off in New mexico (NM) and Texas :~ 4.3 GV

geomagnetic cut-off in Siberia :~ 1 GV

HEAT (balloon)

Apparatus

– Superconductiong magnet
– Drift Tube Hodoscope tracking chamber
– Two layers of scintillators provide TOF
– TRD on top
– EC : measure $e^{\pm}$ and discriminate against hadrons

Physics

– Observation of e^{+} from 1-50 GeV
– Observation of e^{-} from 1-100 GeV
– Observation of $\bar{p}/p$ ratio between 4.5 and 50 GV

Launch : May 1994 from Fort Sumner(NM) and August 1995 and Spring 2000 from Lynn Lake Manitoba

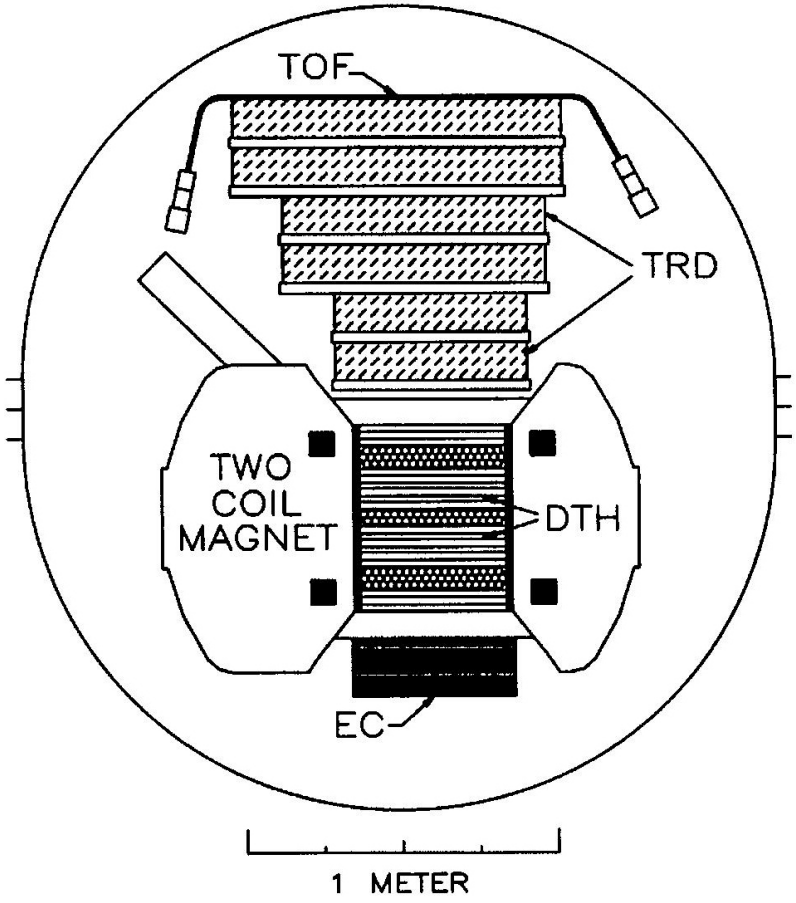

1994 apparatus

CAPRICE (balloon)

Physics

– Study $\bar{p}$ and e^+ in the energy range from few GeV up to tens GeV.
– He between 1-100 GeV/n
– d around 20 GeV/n

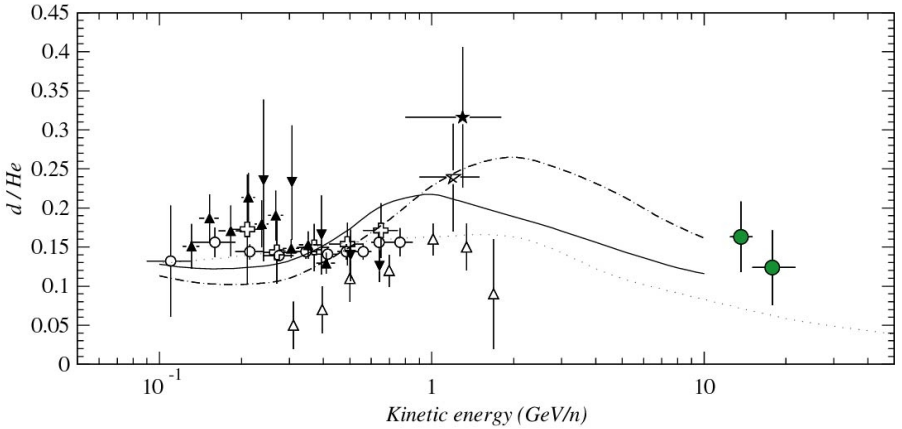

Apparatus

– A drift chamber tracking system placed inside a superconducting magnet.
– a Si-W electromagnetic imaging calorimeter,
– a TOF and a RICH

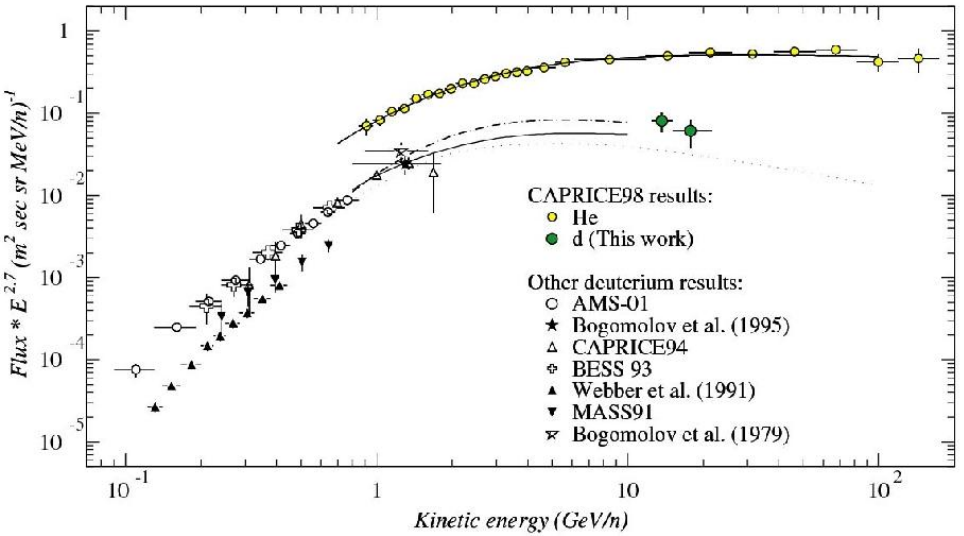

ISOMAX (balloon)

Apparatus

Superconducting magnet spectrometer TOF system and silica-aerogel Cerenkov counters for the velocity determination

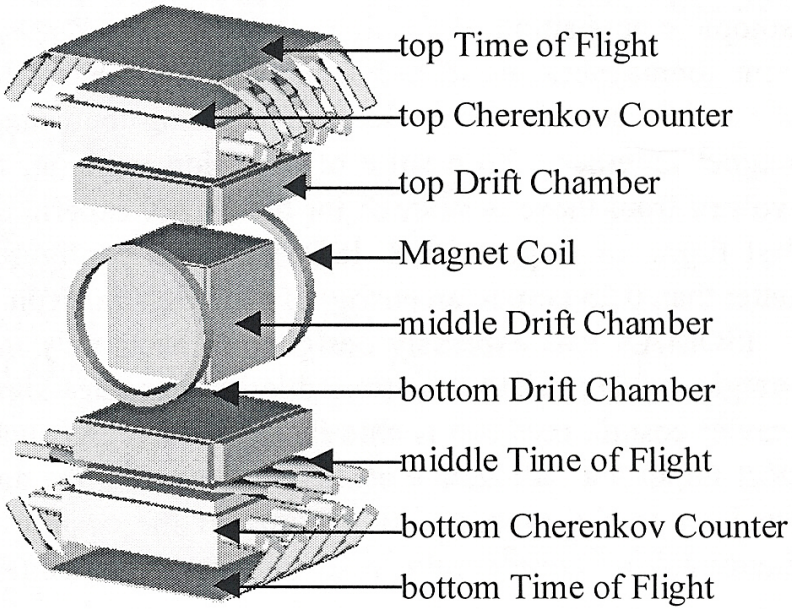

Physics

Isotopic composition of the light isotopes ($3 < Z < 8$) up to 4 GeV/n (1998-13hrs at Lynn lake, $^{10}Be/^{9}Be$)

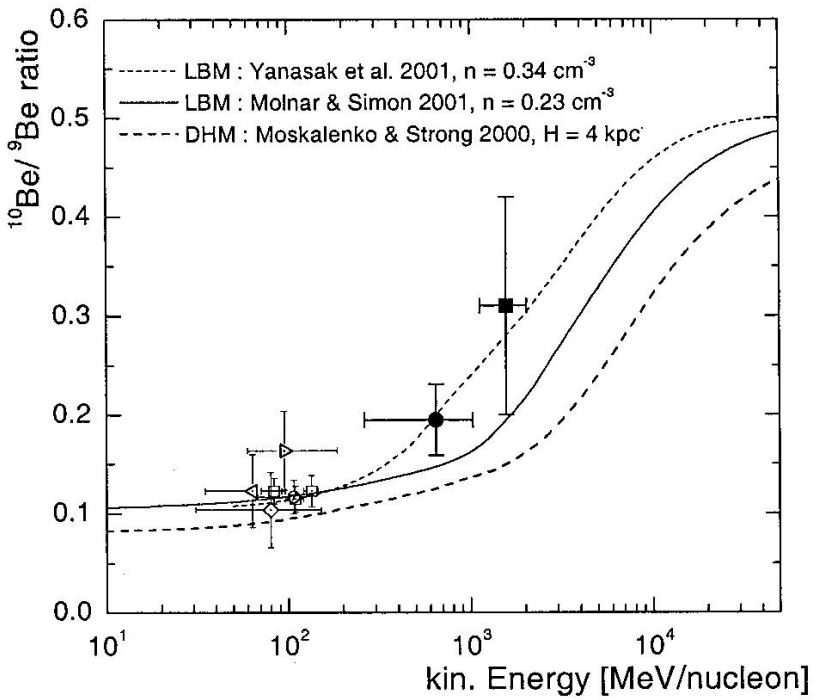

n : mean interstellar gas density

H : height of the halo

TIGER (balloon)

Physics

For ultra-high cosmic rays abundance ($26 < Z < 40$).

Apparatus

4 scintillators, 2 cerenkov detectors and a scintillating fiber hodoscope to determine the charge (Z) and energy of a particle.

31,8 days flight from Mc Murdo base in Antartica, i.e 2 complete round trips around the South Pole in December 2001 with an average altitude of $\sim 35km$.

100 ultra-heavy galactic cosmic-ray (GCR) events with $Z = 31$ and 32

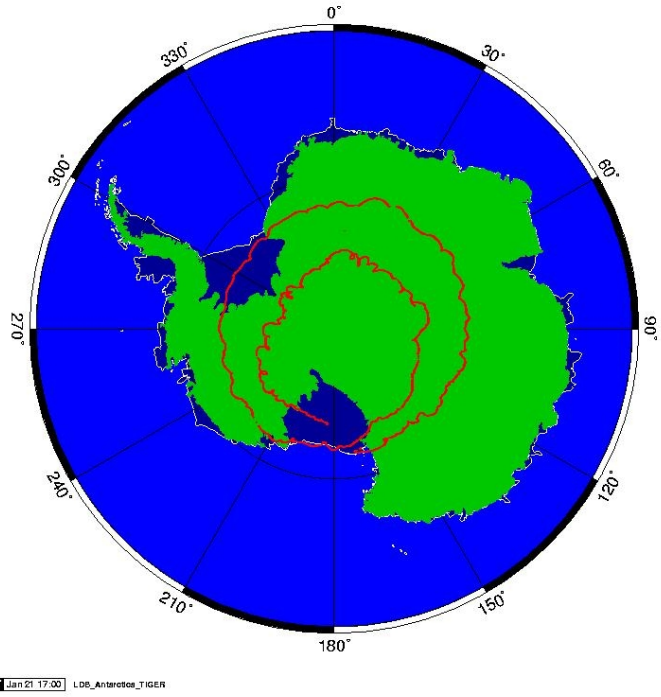

BESS

The BESS instrument (balloon)

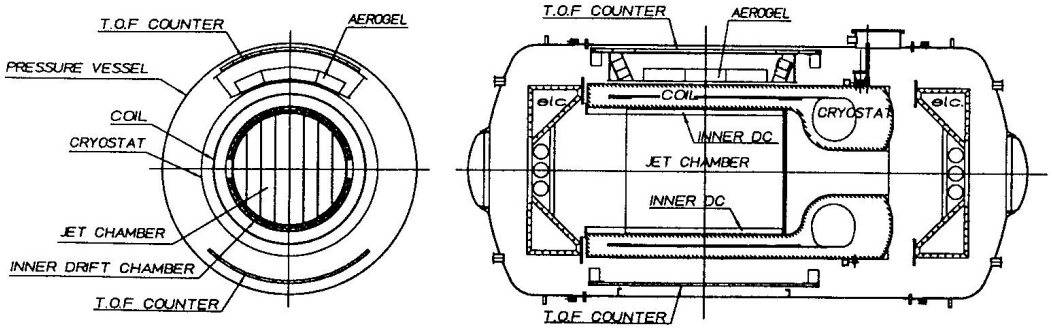

Apparatus

– thin (5g/cm^2) superconductiong coil $B = 1T$, acceptance 0.3 m^2·sr

– jet type + inner drift chambers : 24 points tracking for p measurement ($\sigma_p/p = 0.5\%$ at 1 GeV)

– TOF scintillators ($\sigma_t = 75$ ps) provide dE/dx measurement

– aerogel Cerenkov

– residual air thickness $5g/cm^2$

– floating time $\sim$17 hours over Canada

Physics

– Precise measurement of $\bar{p}$ at low energy

– Antiparticle search ($\overline{He}, \bar{d}$)

– $^3He/^4He$ ratio

BESS Spectrometer Progress

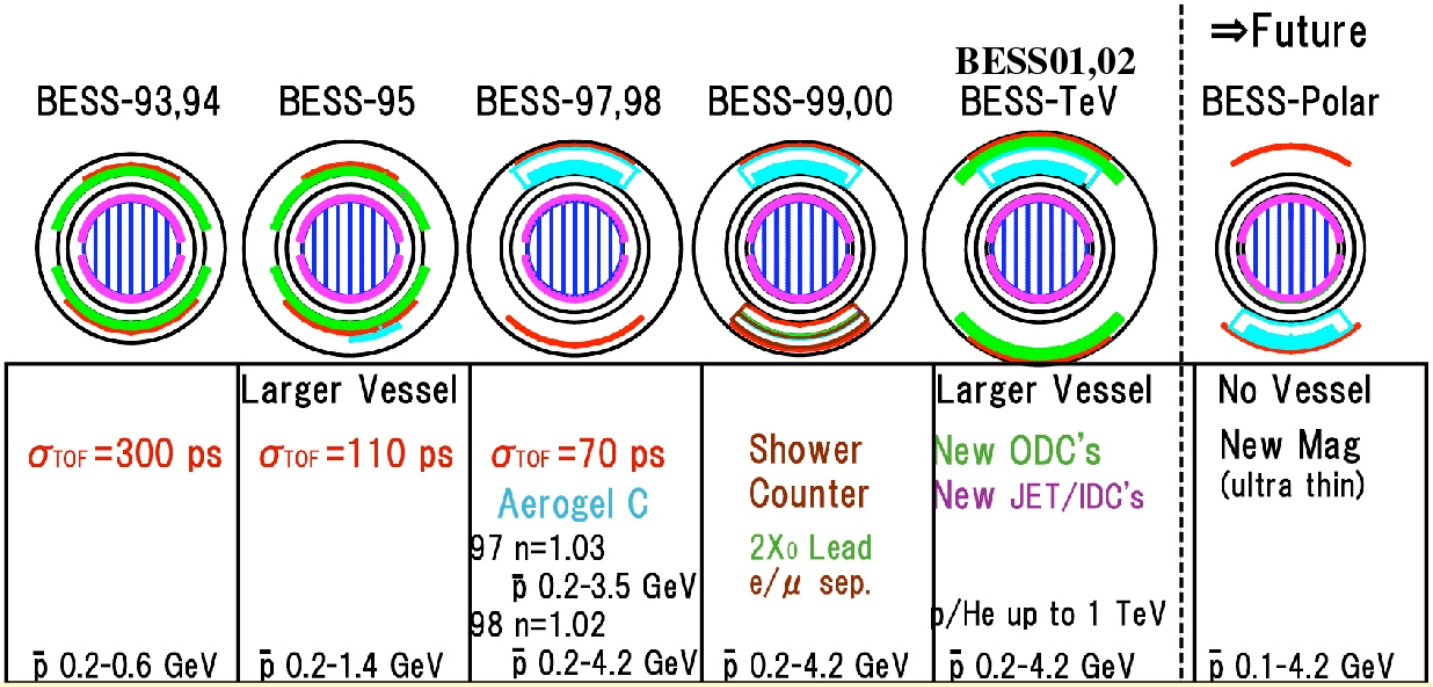

BESS improved in every 9 successful flights

Maximizing advantages in Balloon Experiments

CREAM future detector

100 days mission

Different from those used in prior high-energy experiments in that it employs both a TRD and a hadron calorimeter.

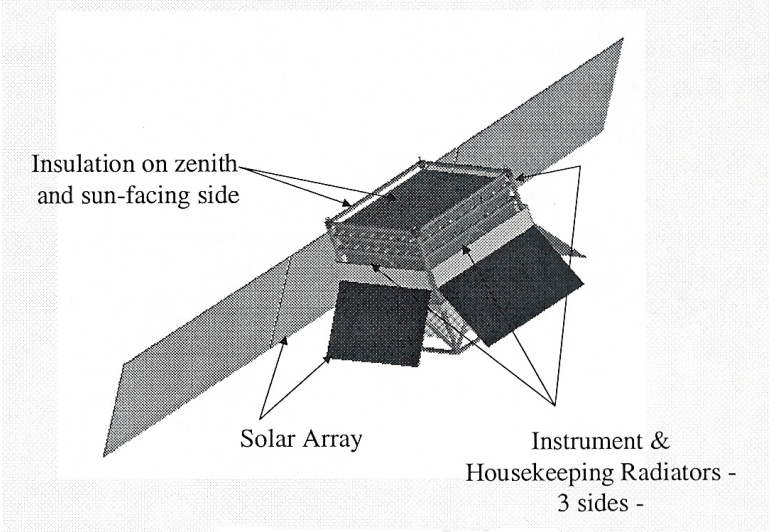

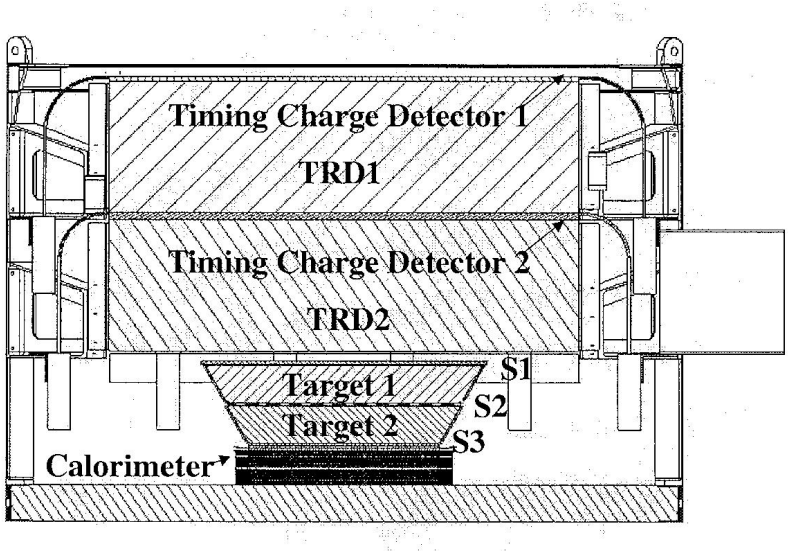

requires detector qualification, reliability and telecommuniaction logistics which are close to space borne experiments (1-2Hz data rate, 140 W)

- a W-scintillator sandwich Calorimeter (0.3 m^2)
- a carbon target with scintillator layers
- a large acceptance TRD (1.3 m^2) to measure heavy nuclei
- a segmented timing-based particle charge detector

Antiproton results

$\bar{p}$ are secondaries produced in collisions of energetic CR nuclei with interstellar material. Their spectrum with a peak at about 2 GeV is distinctly different from other CR species.

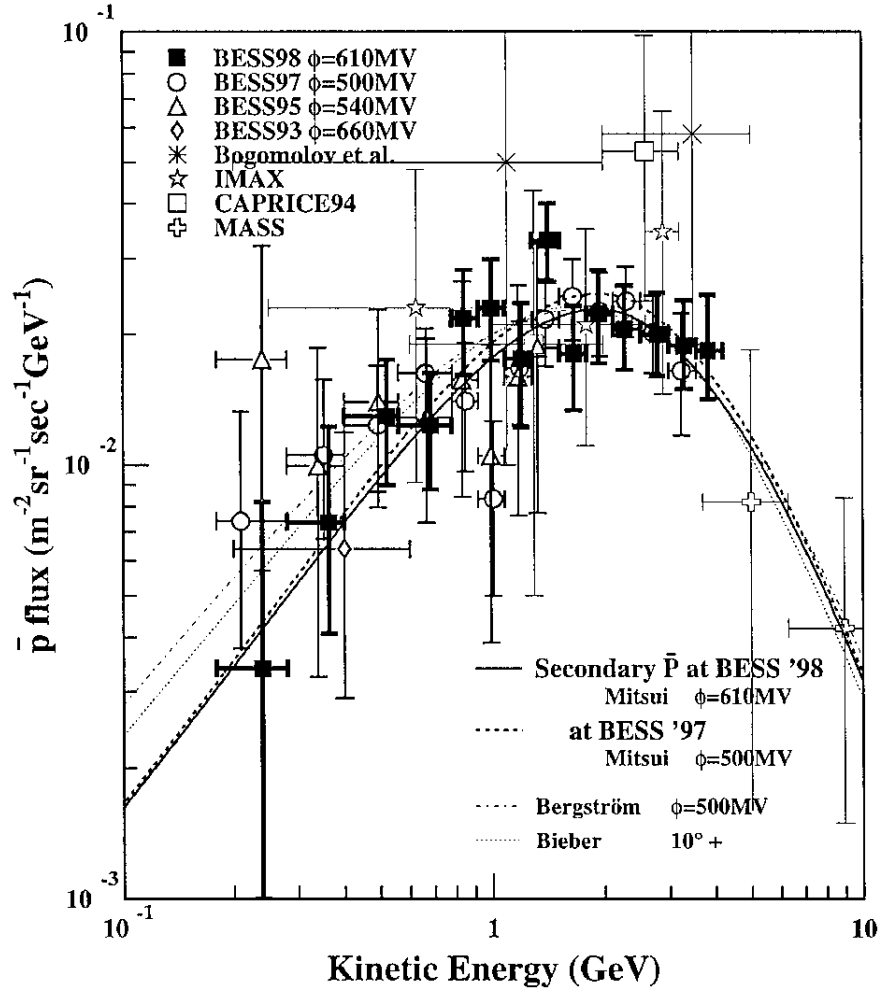

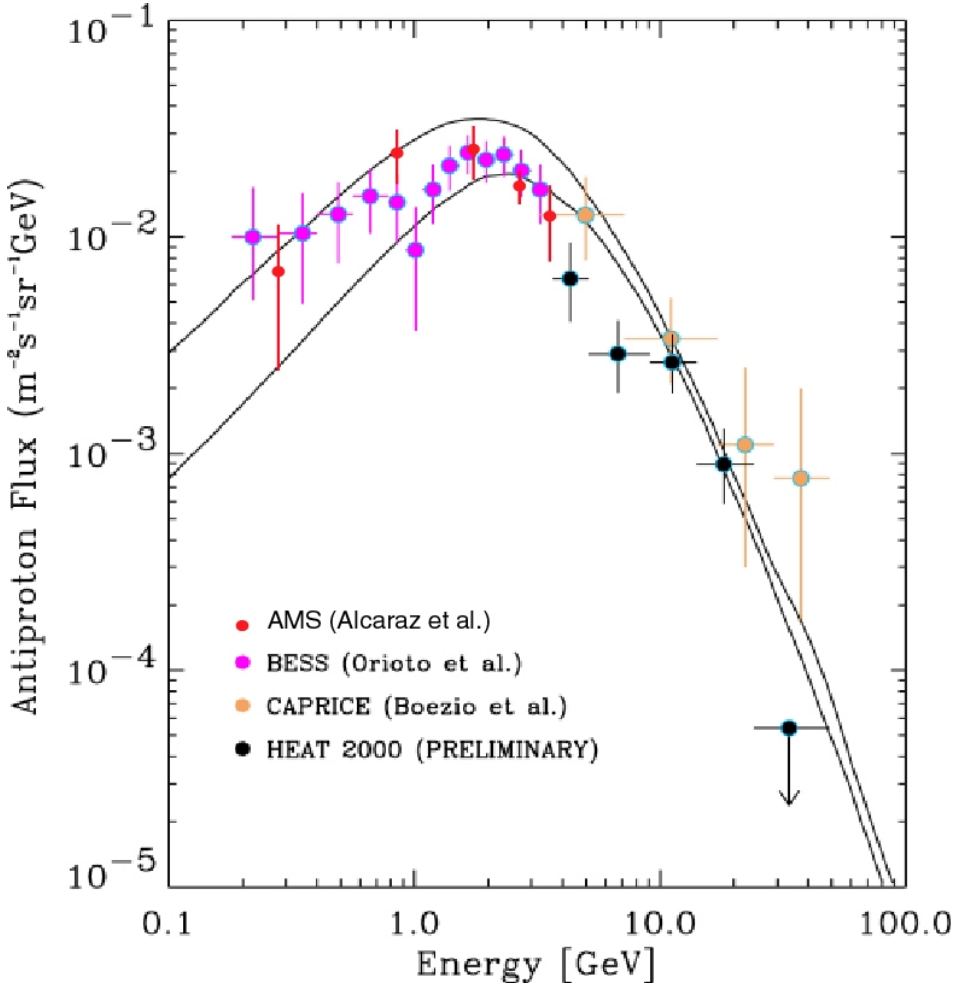

Space experiments

– Space-Experiments already launched

  – CRIS on ACE $launched$ in 1997 orbits around $L1$ point
  – NINA 1 $launched$ in 1998
  – AMS-01 (10 days on $Discovery$) 1998
  – NINA 2 $launched$ in 2000
  – MARIE on Odyssey $launched$ in 2001 in Mars magnetosphere : fluxes with near Earth data within experimental data
  – .....

– Space-Experiments to be launched

  – PAMELA *to be launched* in 2004
  – AMS-02 *to be installed* in 2006 for 3 years of operation on ISS Station
  – .....

The PAMELA instrument (satellite)

apparatus

– Permanent magnet : 0.4 T

– 6 planes of $\sim 16 \times 16$ cm^2 of Si tracker with spatial resolution : 3μm in the bending direction 12 μm in the other direction

– TRD to select electrons out of hadrons up to ~ 1000 GeV

– Imaging calorimeter made of silicon sensor planes interleaved with tungsten absorbers.

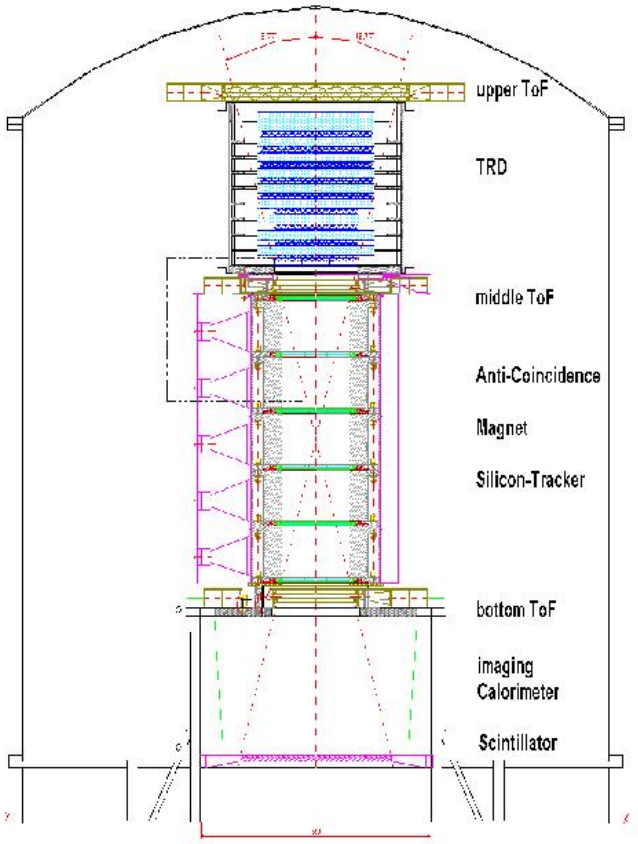

Physics

– $\bar{p}$:80 MeV-190 GeV ($> 3 \times 10^4$)

– e^+ : 50 MeV-270 GeV($> 3 \times 10^5$)

– Search for antinuclei : $\overline{He}/He \sim 7 \times 10^{-8}$

– Nuclei spectra (from H to C) : 80 MeV/n-350 GeV/n

– p, 80 MeV-700 GeV (3×10^8)

– e^- : 50 MeV-2 TeV (6×10^6)

The PAMELA instrument (satellite)

Polar orbit 690 km ∼2004

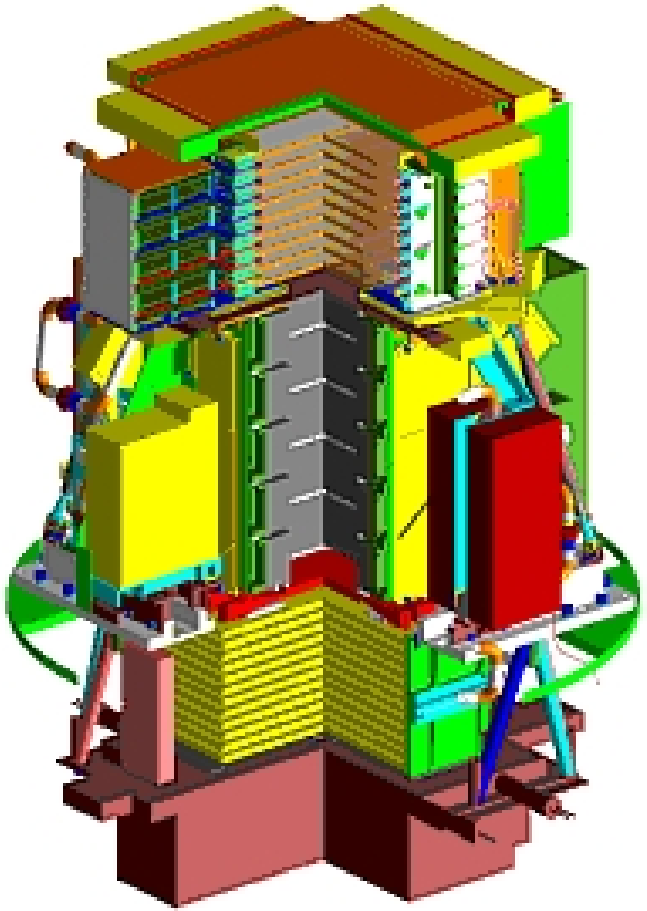

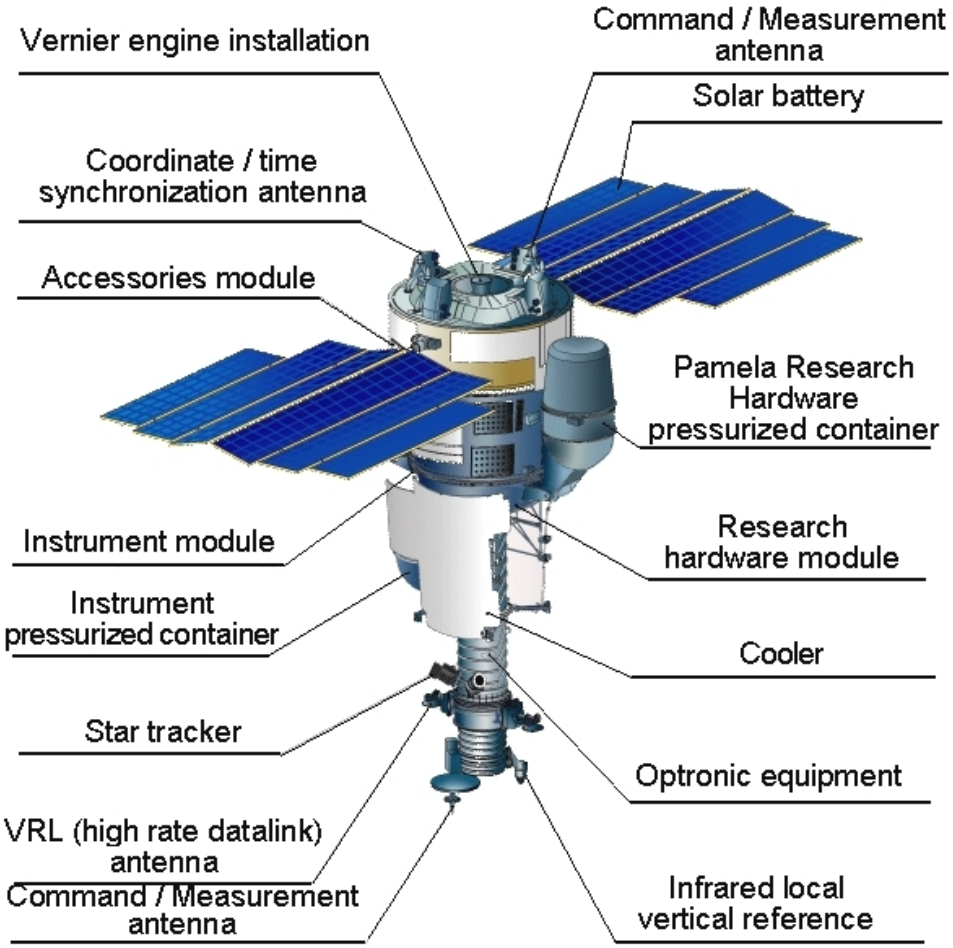

PAMELA-BESS-AMS-02

Project	BESS-Polar	PAMELA	AMS-02
Acceptance ($m^2 \cdot$ sr)	0.3	0.002	0.5
MDR (GV)	150	740	2500
Flight duration (days)	20	1000	1000
Flight Altitude (km)	36	690	350
Residual Air (g/cm^2)	5	-	-
Weight (tons)	1.5	0.38	~ 7
Power consumption (W)	600	345	2000
Magnetic field (Tesla)	0.8-1	0.4	0.87
Flight latitude (deg.)	80	$\pm$70	$\pm$52
Energy region (GeV)	> 0.1	> 0.1	$>\sim$0.5
Flight vehicule	Balloon	Satellite	ISS

PAMELA-BESS-AMS-02

	MDR (TV)	Exposure ($days$)	Aperture $(cm^2\ sr)^{-1}$	Sensitivity / # of events	Range $(GeV)(GeV/n)$
$Pamela$	0.75	1000	20.5		
$(2004-2007)$			p	3.10^8	$0.080-700.$
			$\bar{p}$	3.10^4	$0.080-190.$
			e^-	6.10^6	$0.050-2000.$
			e^+	3.10^5	$0.050-270.$
			$He-C$		$0.080-350.$
			$\bar{He}/He$	7.10^{-8}	
$BESS\ Polar$	0.2	$10+20$	3000		
$(2004-2007)$			p	3.10^9	$0.200-200.$
			$\bar{p}$	3.10^4	$0.200-4.$
			He	4.10^7	$0.200-200.$
			$\bar{D}/D$	10^{-5}	$0.100-0.700$
			$\bar{He}/He$	3.10^{-8}	
$AMS-02$	2.5	1000	5000		
$(2006-2009)$			p	2.10^{10}	$0.500-2500.$
			$\bar{p}$	3.10^6	$0.500-400.$
			e^-	6.10^8	$0.500-5000.$
			e^+	3.10^7	$1.-400.$
			$He-Fe$		$0.500-1400.$
			γ		$2.-300.$
			$\bar{D}/D$	3.10^{-7}	
			$\bar{He}/He$	1.10^{-9}	

AMS-01 Pilot Exp't : STS91, June 2-12, 1998

– Principle goal : resupply MIR and crew exchange
– Qualification and test mission for AMS-01
– 90 hours of dedicated data taking
– Variable attitudes and altitudes (320-390 km)
– Latitudes $\pm 51.7^{\circ}$, all longitudes
– Detector functioned without faults
– 10^8 events registered
– Measurement of primary flux $e^{\pm}$, p and $\bar{p}$, D, He and $\overline{He}$, heavy ions and anti-heavy ions.
– detection of secondary fluxes geomagnetic field effect
– antimatter sensitivity extended $\overline{He}/He \sim 10^{-6}$
– Six publications (`http://ams.cern.ch/AMS/Publications`)

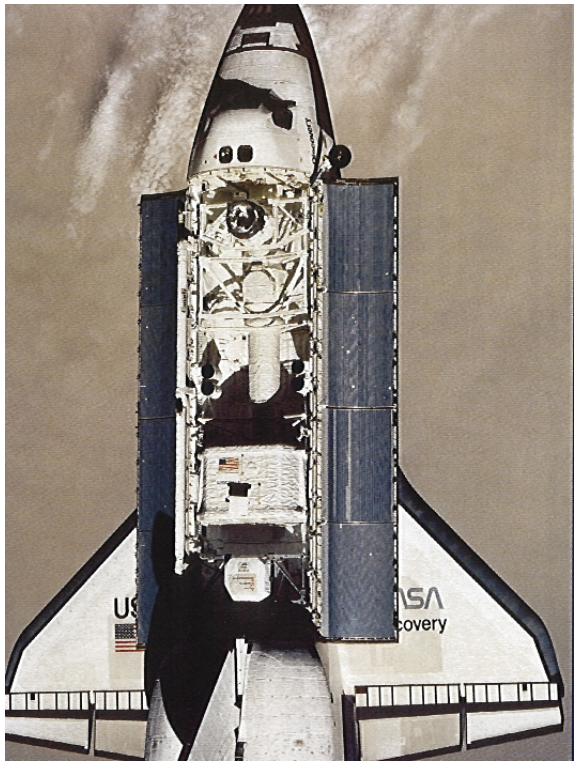

AMS-01 proton

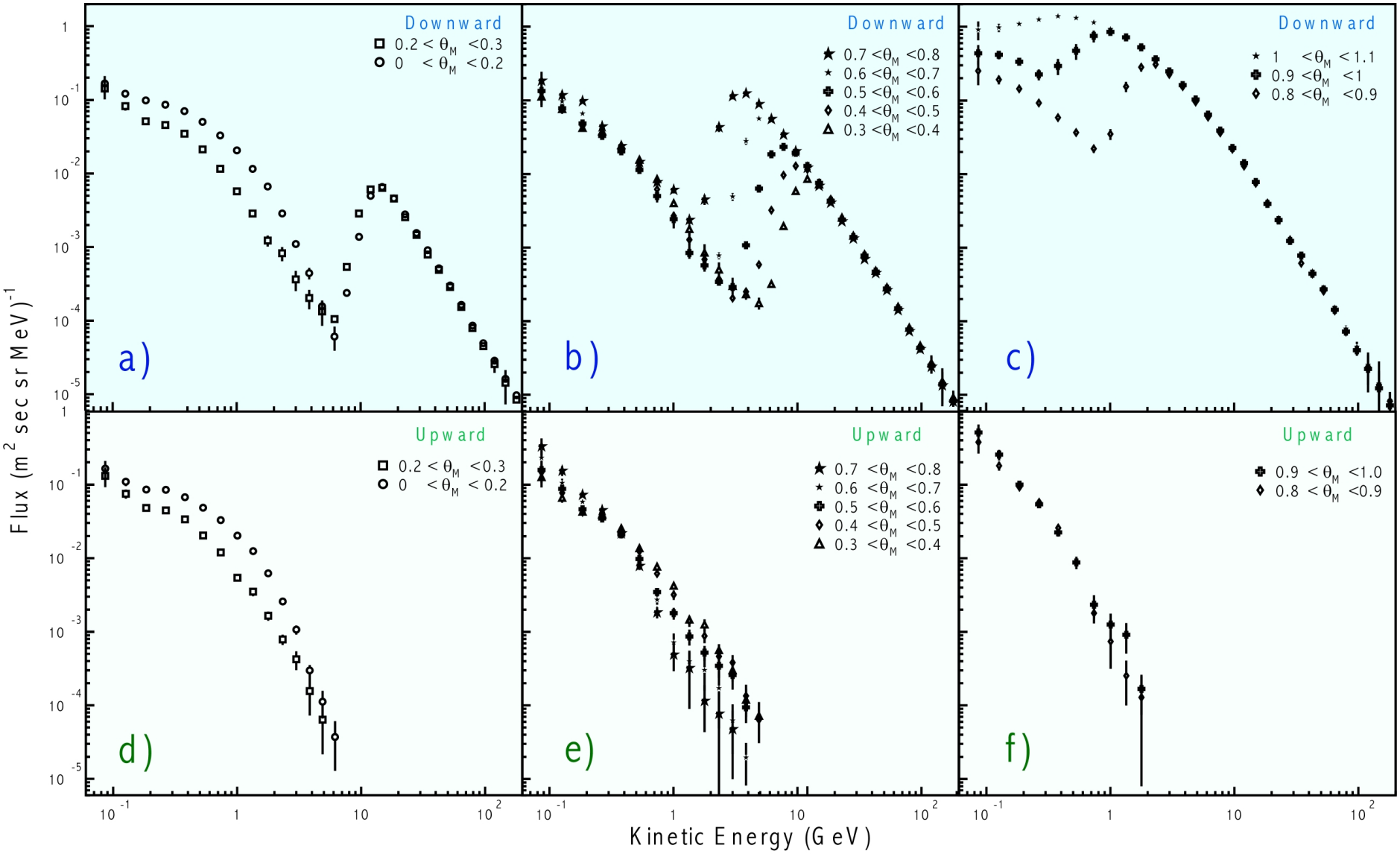

AMS-01 : Search for Anti-Helium

Phys. Lett. B461 (1999) 387

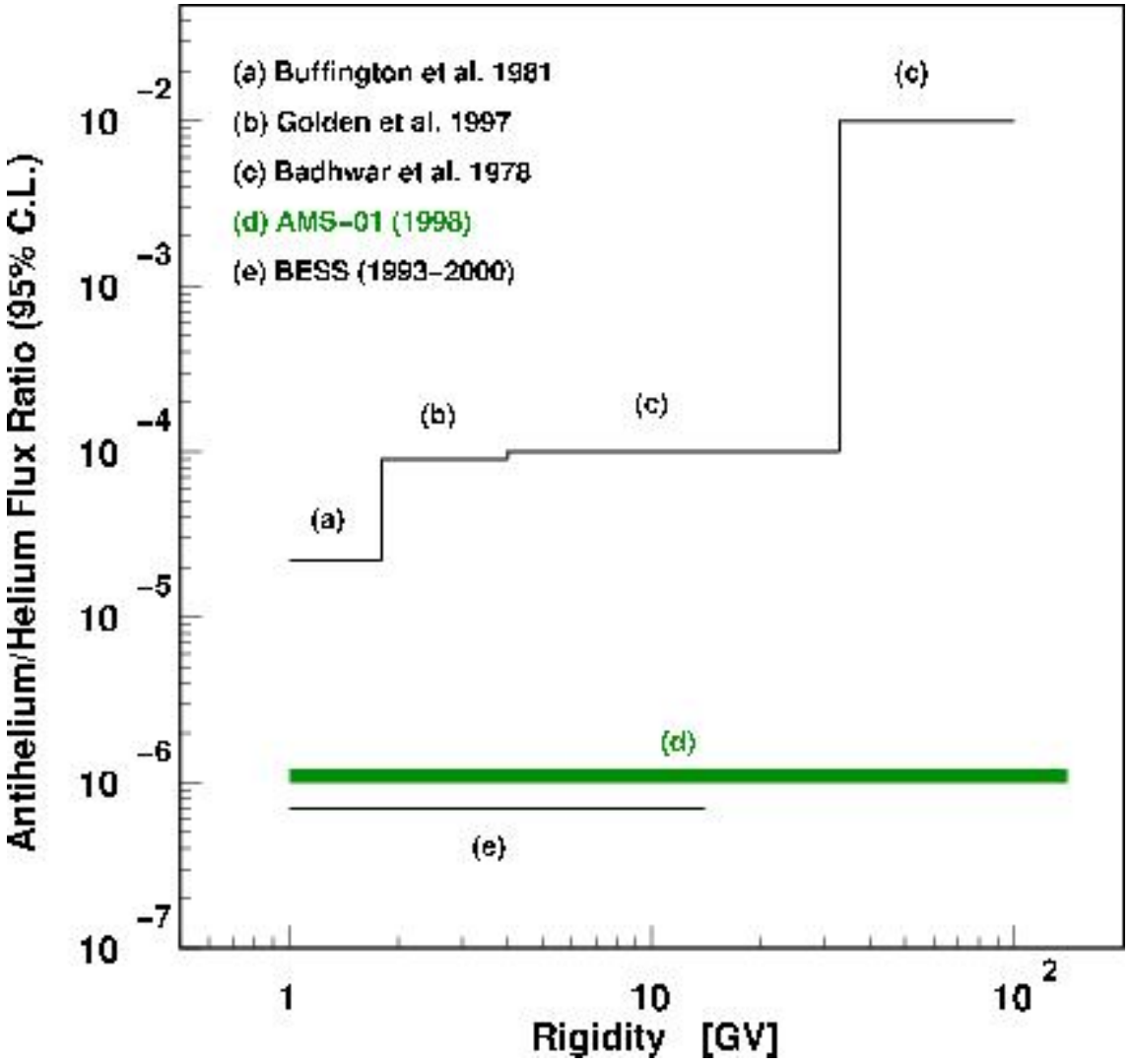

Conservative limit : minimum of acceptance applied to whole rigidity interval

AMS-02

Physics issues

– Search for Cosmic Antimatter
– Search for Dark matter
– Precision measurements of the relative abundance of different nuclei and isotopes of primary cosmic rays
– Gamma ray Astrophysics

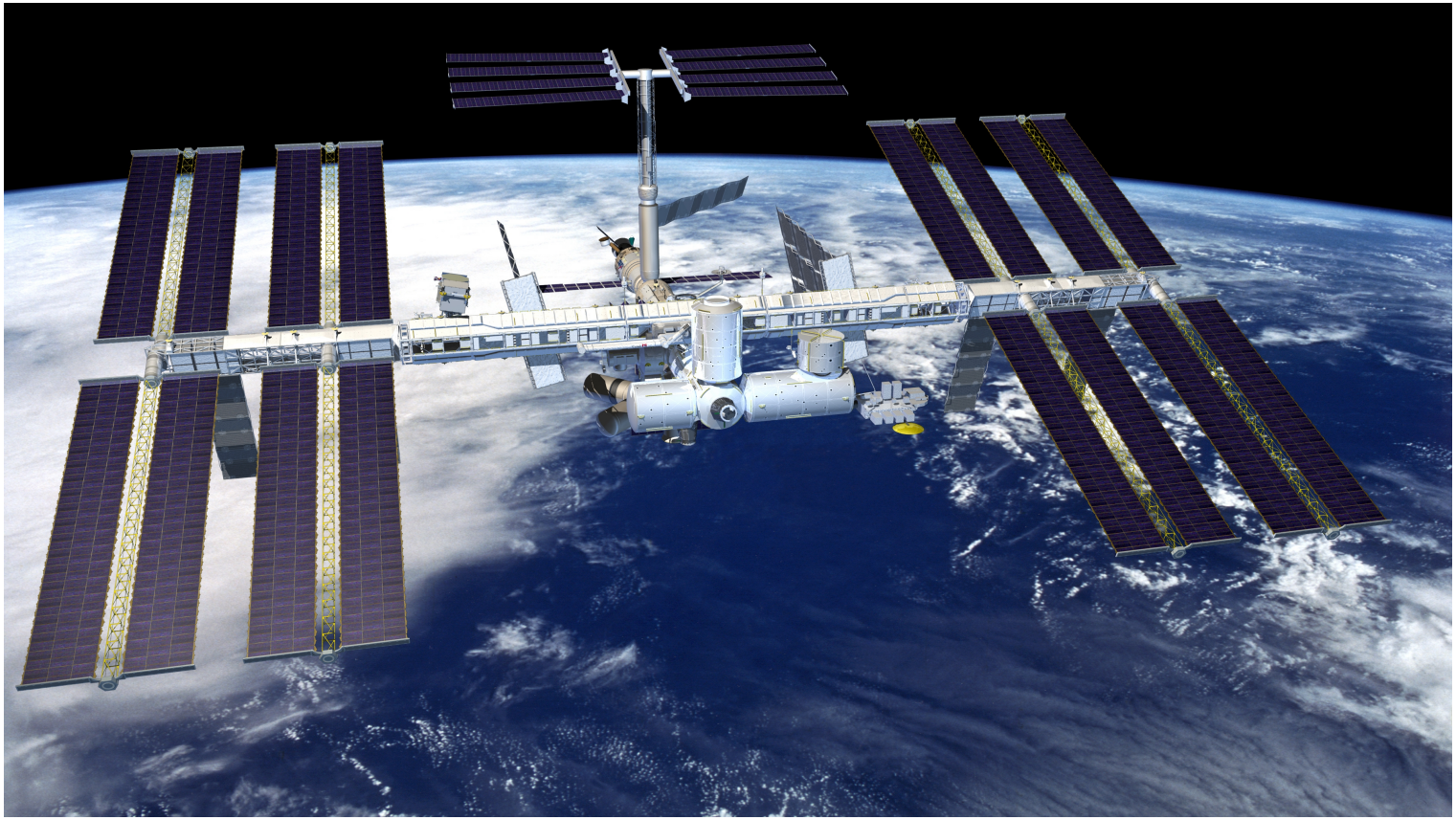

AMS: A TeV Magnetic Spectrometer in Space

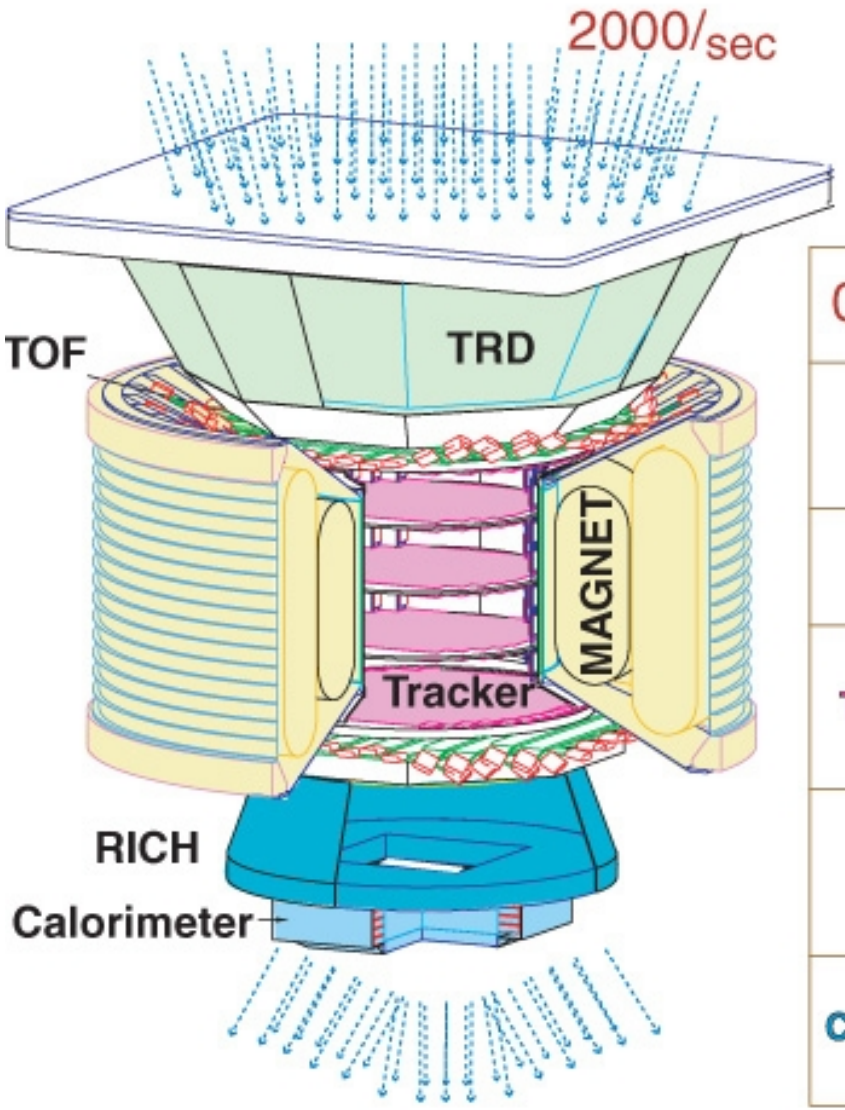

0.3 TeV	e^-	e^+	P	$\bar{He}$	γ
TRD					
TOF					
Tracker					
RICH					
Calorimeter					

y2K025 _5 Gamma

AMS 02

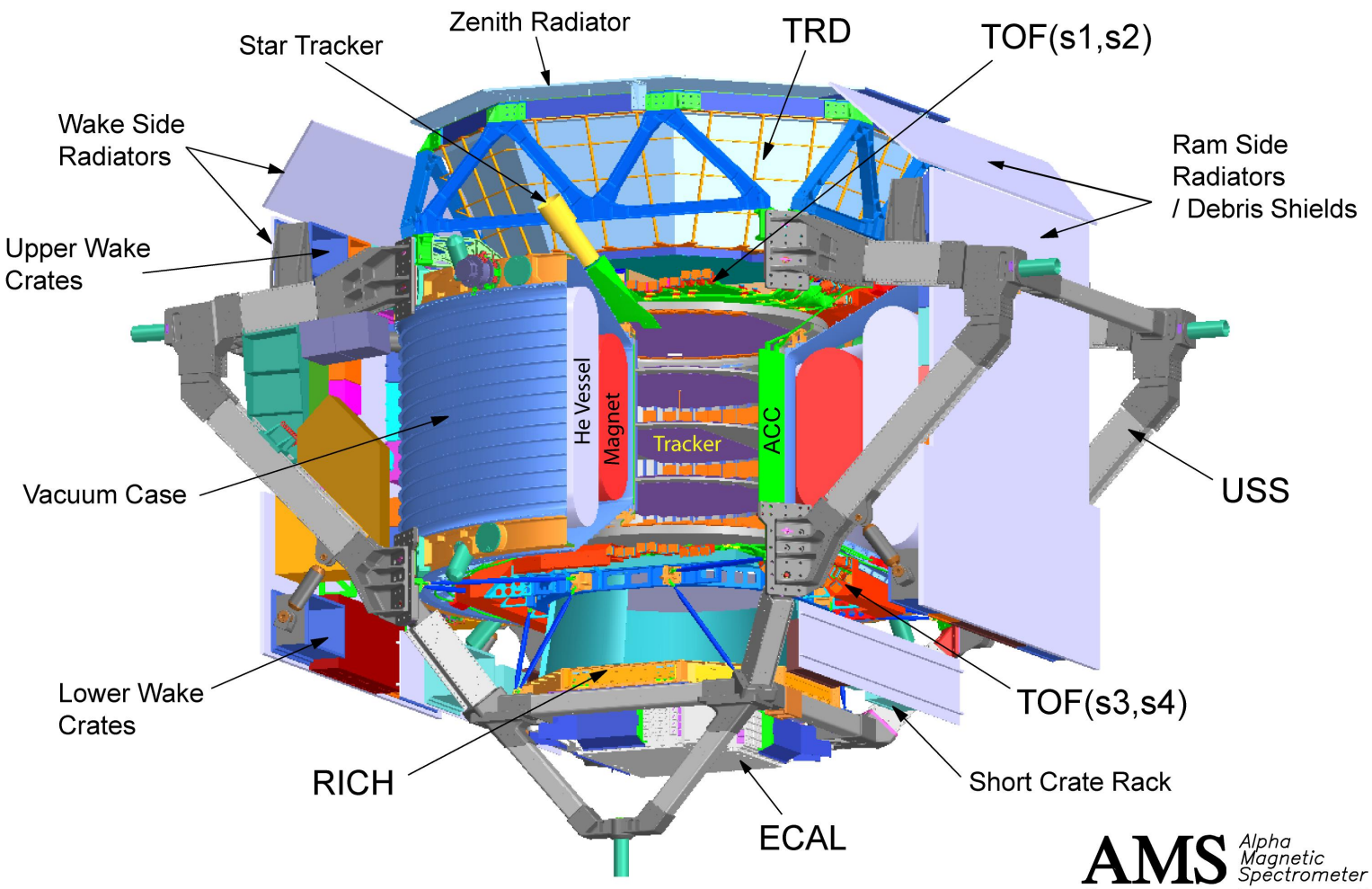

R.Becker 09/05/03

AMS Alpha Magnetic Spectrometer Integration MIT

RB0305AMSposter

AMS-02 : Superconducting Magnet

Construction

– 14 superconducting coils cooled by superfluid Helium at 1.8 K
– geometrical configutation to ensure total dipole moment =0
– Reservoir for ∼3 years of operation without refill (2500l)
– Dimensions : same inner diameter as AMS-01 (1.1m),
– weight : 2360 Kg

It provides

– Central magnetic field ∼ 0.87T, six times AMS-01
– Measurement of rigidity extended up to few TV

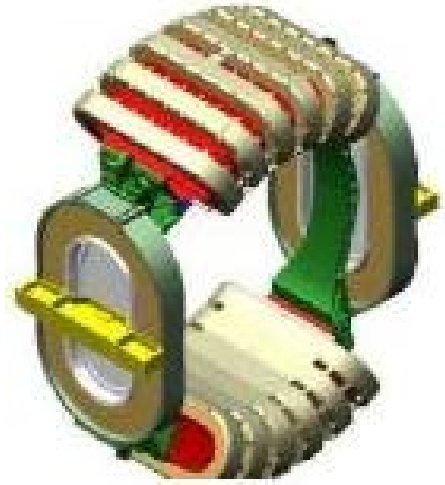

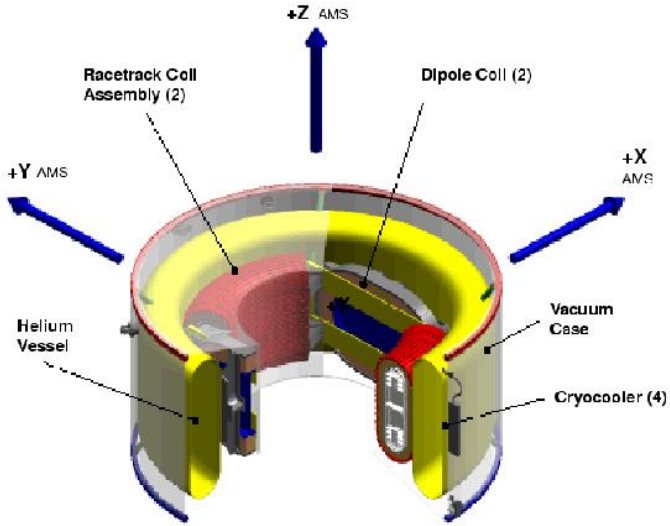

AMS-02 : Tracking Detector

Construction

– 5 ultra light supporting planes (3 inside the magnet and 2 outside)
– 8 layers of double sided silicon microstrip sensors ($\sim 7\text{m}^2$)
– a total of ~ 2500 sensors arranged on 192 ladders
– 7-15 sensors per ladder

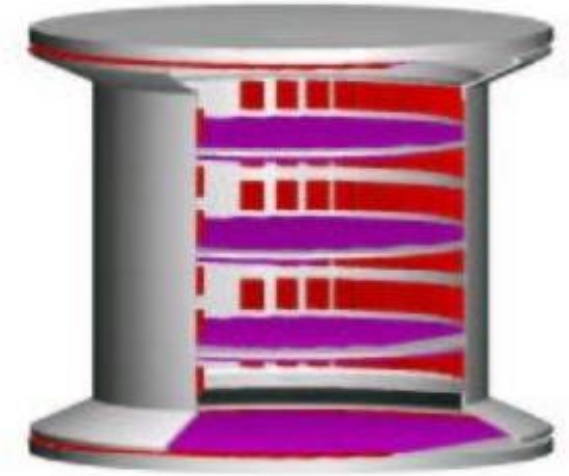

It provides

– 8 independent position measurements of the particle
– particle rigidity ($R \equiv \frac{pc}{|Z|e}$) from track reconstruction up to a few tens of TV
– electric charge (Z) from energy deposition $dE/dx \sim |Z^2|$
– Resolution $\sim$10μm in bending direction, $\sim$30μm orthogonal
– Measures direction and energy of converted photons

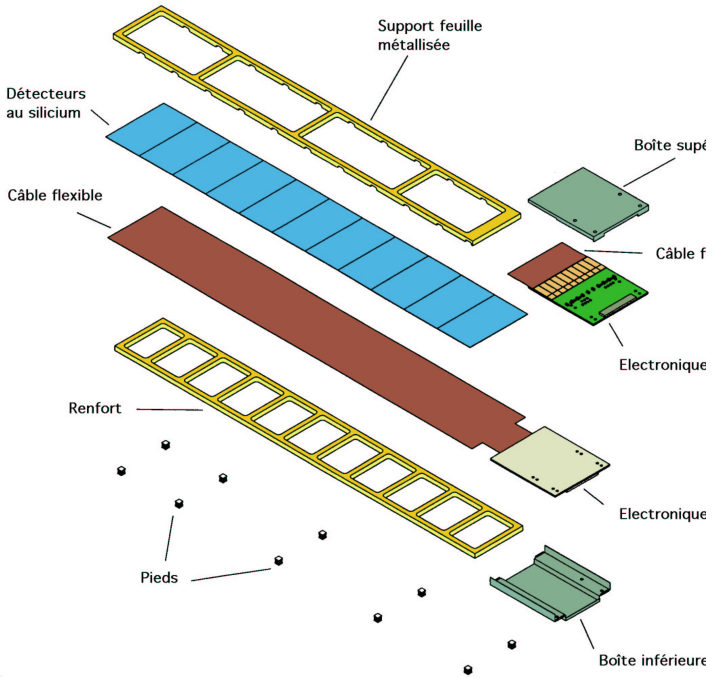

AMS Tracker Plane during Metrology

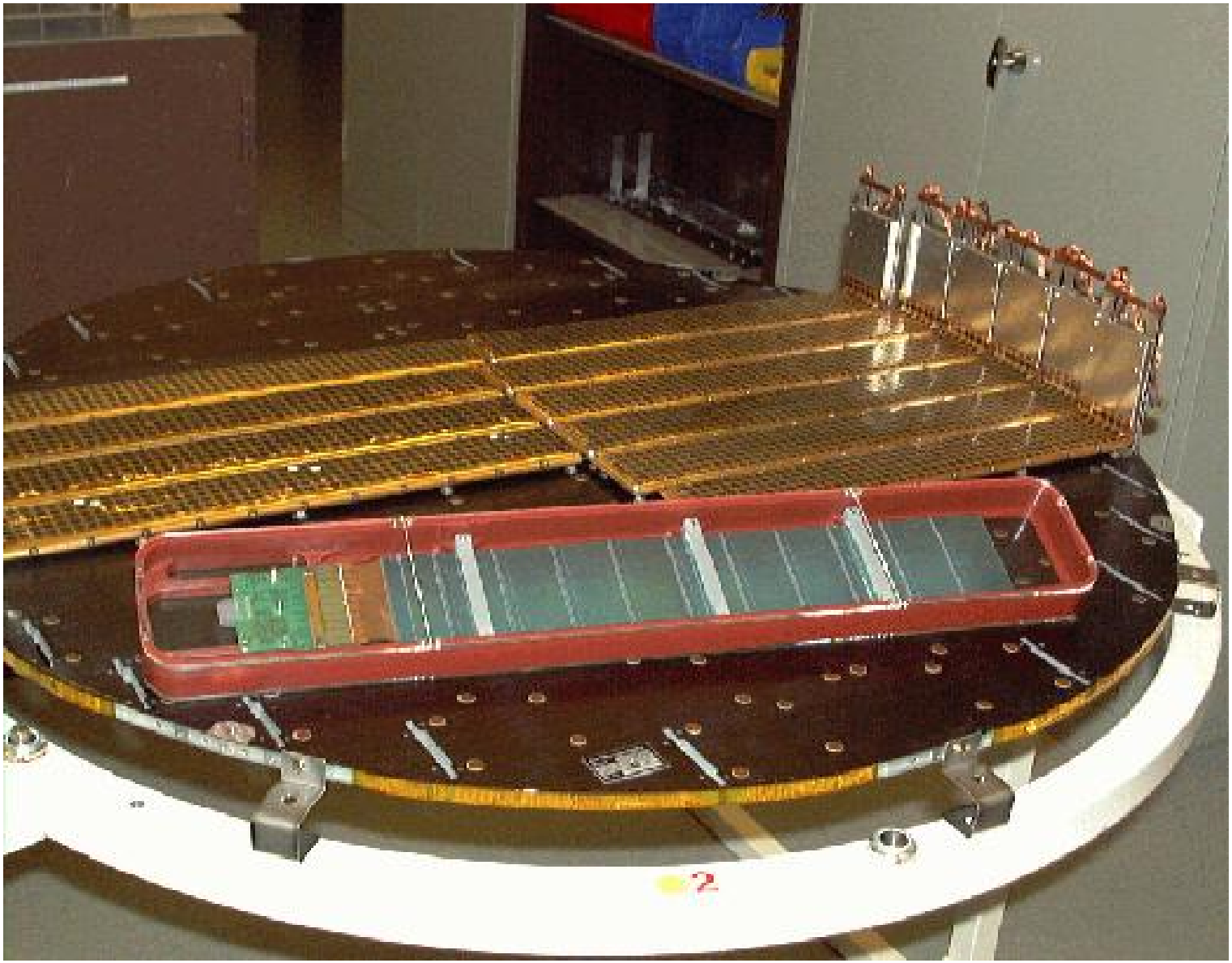

AMS-02 : Transition Radiation Detector

Construction

– modules (328) made of fleece radiator and straw tubes
  – 16 straw tubes per module
  – radiation thicknesss of 23 mm
  – straw tubes ($\phi = 6mm$) filled with Xe/CO_2
– 20 layers assembled on a octogonal shape (total thickness 60 cm)

It provides

– Separate hadrons from electrons up to 300 GeV
– dE/dx
– Helps in tracker reconstruction pattern recognition

Principles

Charged particles with γ Lorentz factor ($\gamma > 10^3$) radiate X-rays upon change in index of refraction,
E_γ= 4-8 keV for e^-

Emission probability small (10^{-2}) $\longrightarrow$ multilayer radiator

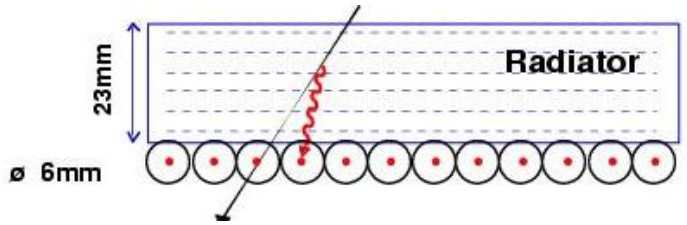

AMS-02 : Transition Radiation Detector

– Need many interfaces, but the soft-X-rays should not be absorbed in the radiator $\longrightarrow$ compromise
– To detect soft X, you need a material with large Z and if possible a large gain (noble gaz) if one detects with a gaz (photo electric effect). One takes $Xe, Z = 54$
– The charged particle ionized also the X-ray detector. One must maximize the ratio (X-ray detection)/(ionisation by the charged particle)
– One single measure does not allow to decide for sure of the presence or absence of radiation transition. You need many measurements $\longrightarrow$ one piles-up detectors

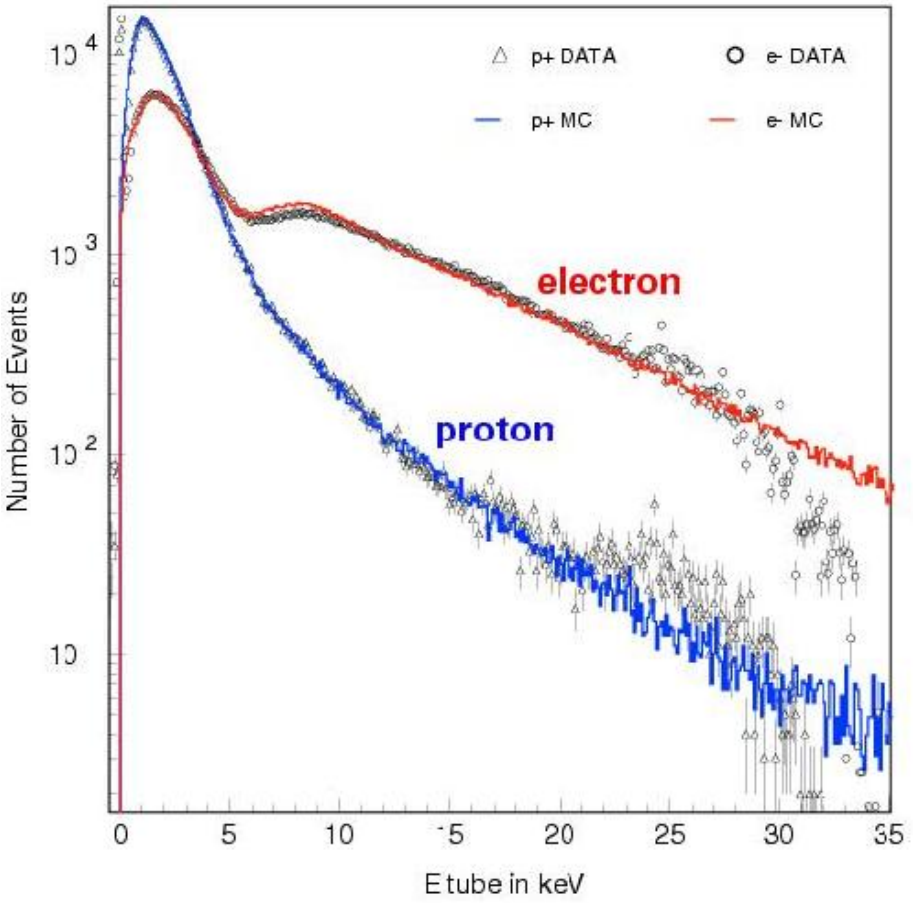

AMS-02 : Time-of-Flight Detector

Construction

– 4 scintillator planes, 1.6 m^2/plane
– a total of 34 scintillator paddles
– 2/3 photomultipliers at both ends
– light guides twisted/bend to minimize magnetic fiels effects

It provides

– Principal fast trigger in 200 nsec
– upward/downward particle separation (10^{-9})
– time-of-flight (resolution $\sim 140psec$), velocity β and direction
– Z from dE/dx, $\Delta E/E$ $\sim$10% for MIPS $\rightarrow$Z

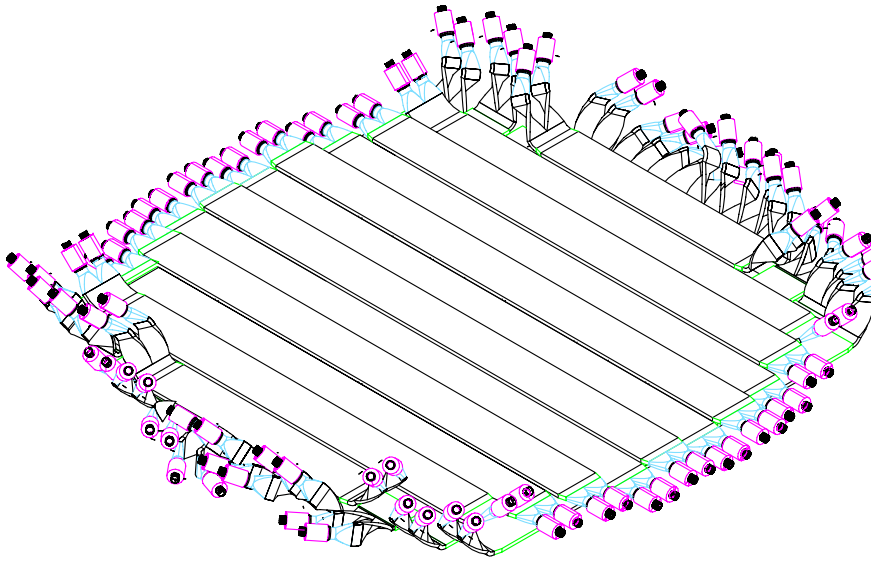

AMS-02 : Ring Imaging Cerenkov Detector

Construction

– proximity focusing Ring Imaging Detector
– 2 different solid radiator configuration
  aerogel ($n \sim 1.03, 3cm$ thichness)
  sodium fluoride ($n \sim 1.33, 0.5cm$ thickness)
– conical reflector
– photomultiplier matrix
  680 multipixelized (4×4) detectors
– spatial pixel granularity : $8.5 \times 8.5\ mm^2$

It provides

– Cerenkov light emission for $v > c$ in radiator
– Photon detection on a circle
– velocity from emission angle
  $\Delta\beta/\beta \simeq 10^{-3}$
– Redundant particle mass measurement
– Z up to Fe, $\Delta Z \sim 20\%$
– albedo rejection
  directional sensitivity

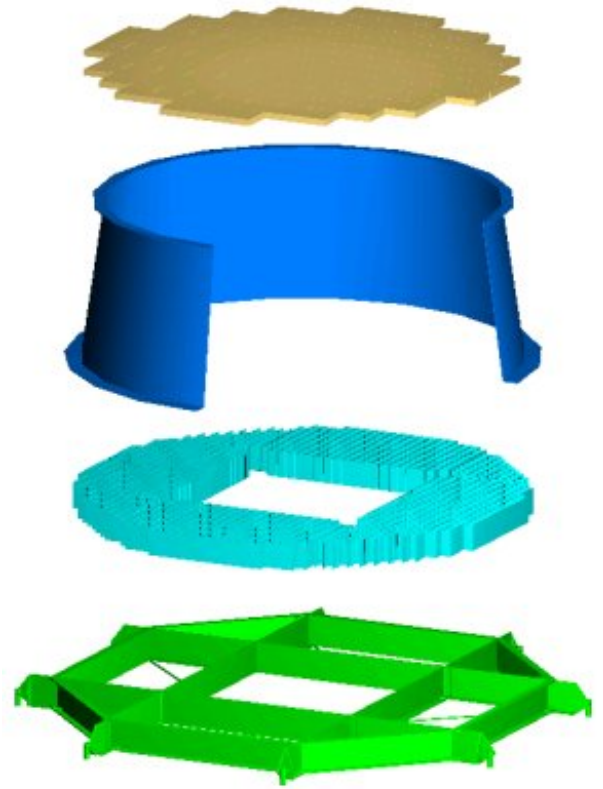

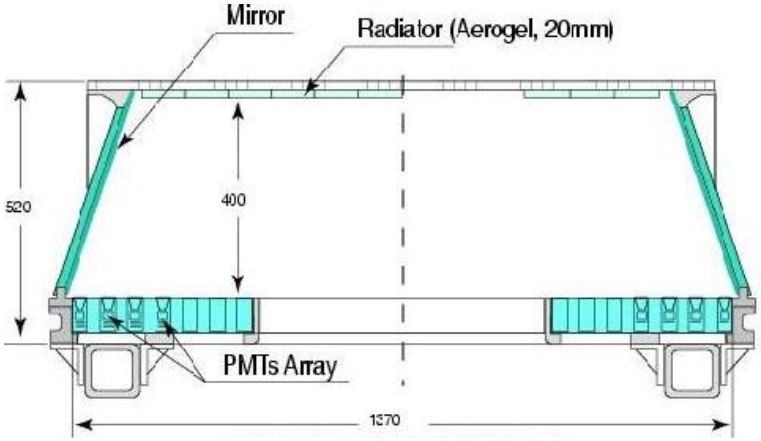

AMS-02 : Ring Imaging Cerenkov Detector

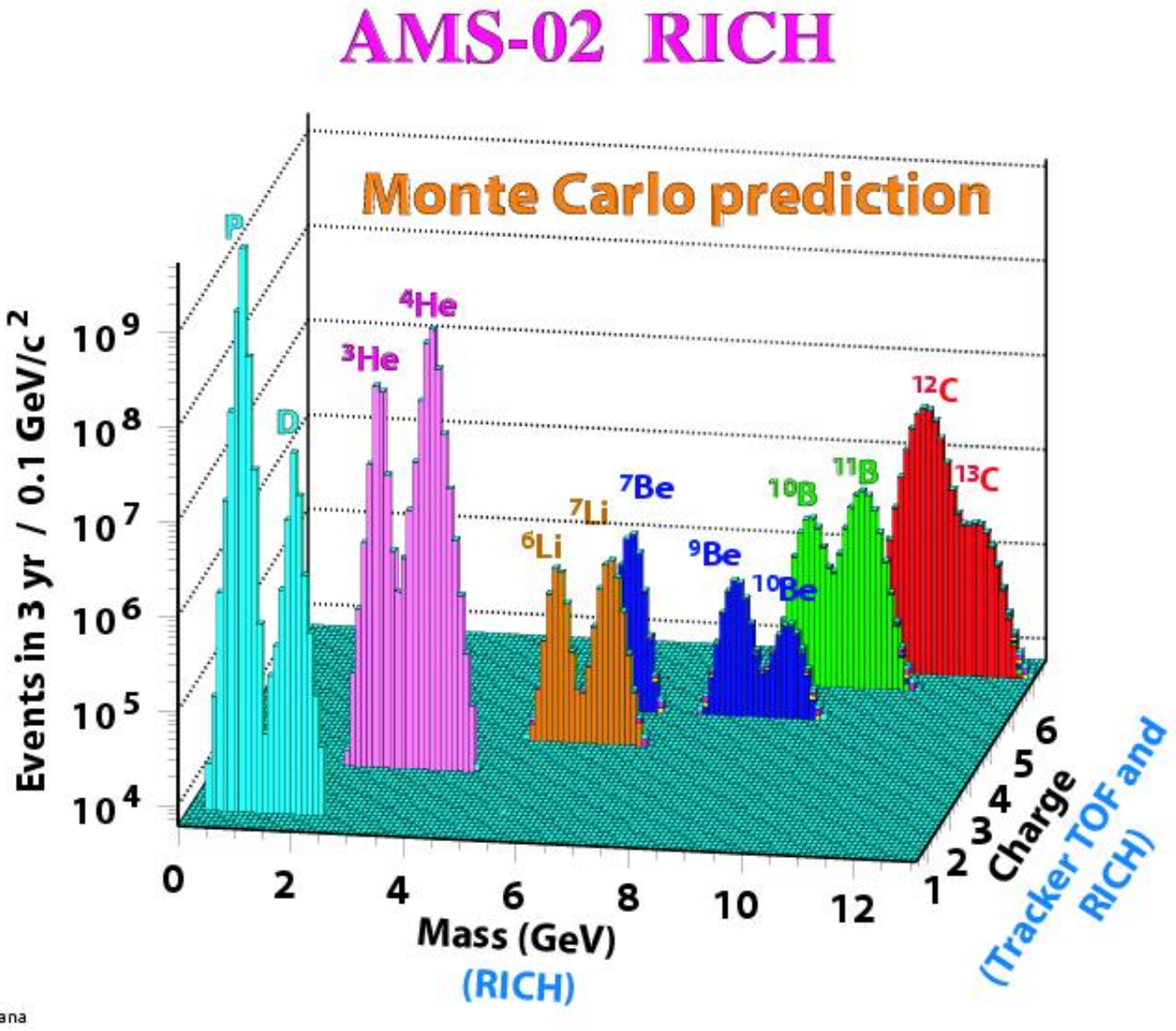

AMS-02 : Ring Imaging Cerenkov Detector

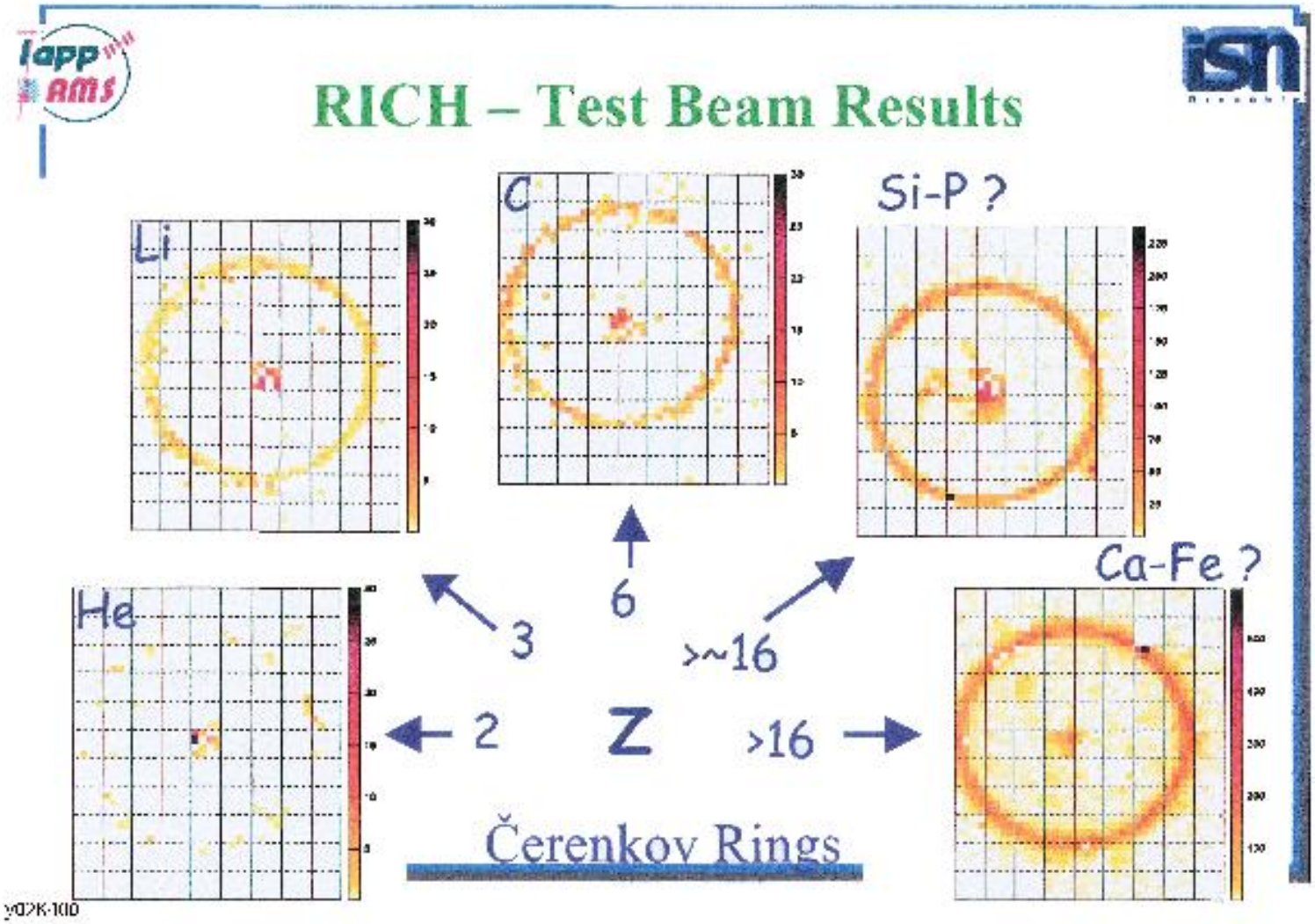

AMS-02 : Electromagnetic Calorimeter

Construction

– Lead-scintillating fibers sandwich
– 9 superlayers piled up disposed alternately along X and Y
– $\sim 18 X_o$ radiation length
– 3D sampling by crossed layers, read out with 384 4-pixel PMTs

It provides

– $e^{\pm}, \gamma$ energy measurement
$\delta E/E$
$\simeq (12 \pm 0.4)\%/\sqrt{E} \oplus (2.8 \pm 0.1)\%$
– Distinction between hadrons and e/γ by shower shape
– Protons supressed by 10^{-4} from 10 to 300 GeV. Together with TRD, rejection of hadrons/electrons $\geq 10^6$
– Independent photon detector, angular resolution $\sim 1^\circ$

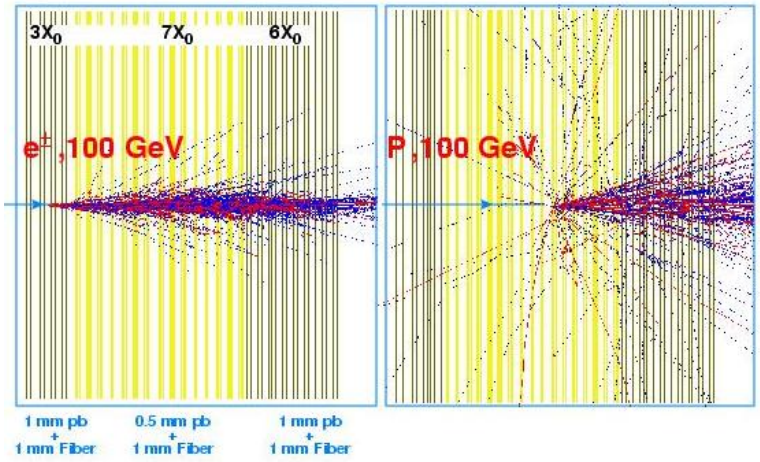

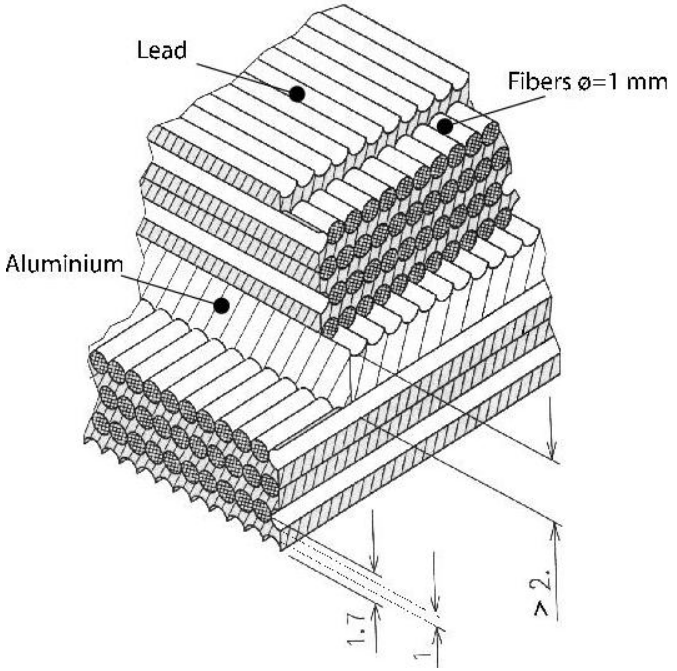

Isotopic components from AMS-02

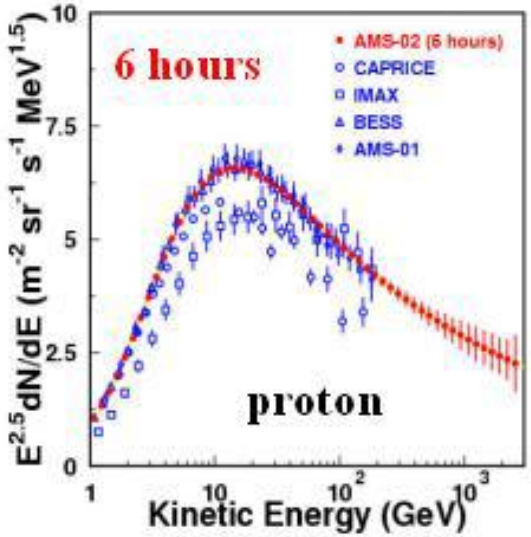

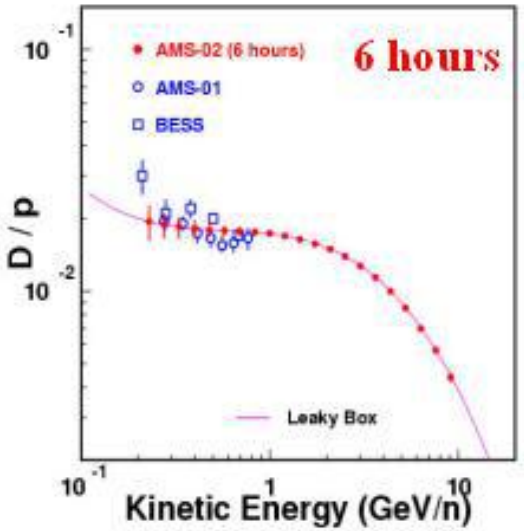

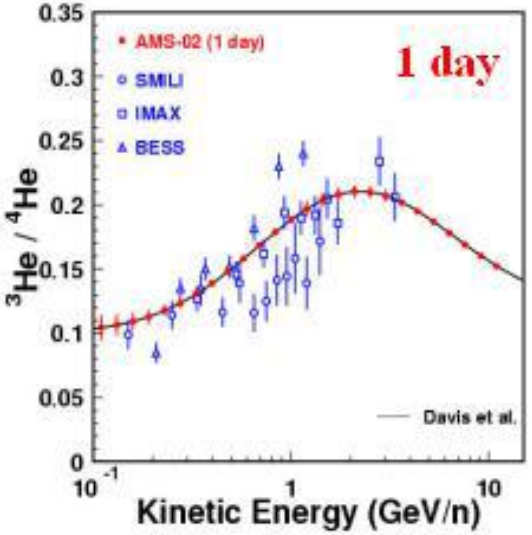

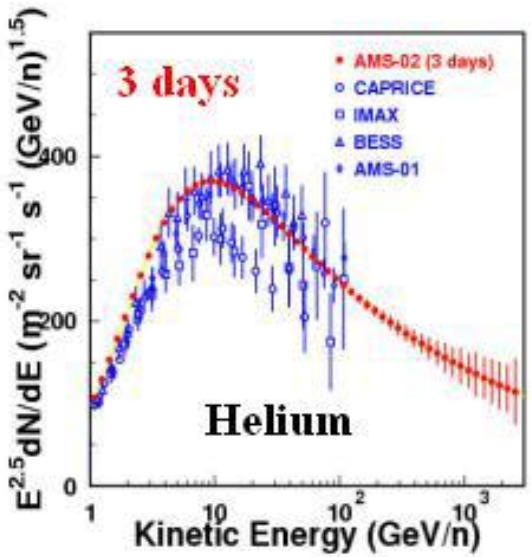

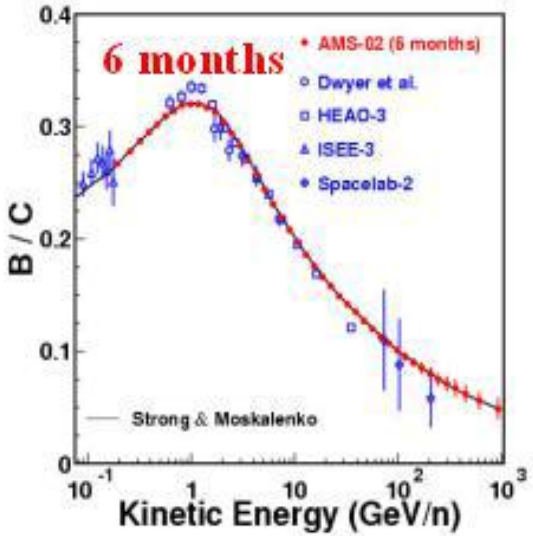

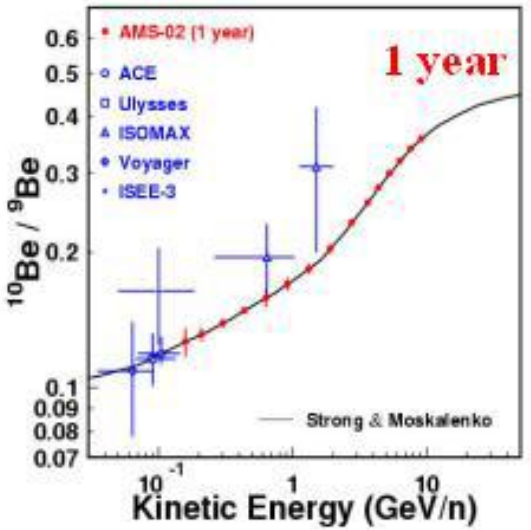

AMS-02 : Search for Antimatter

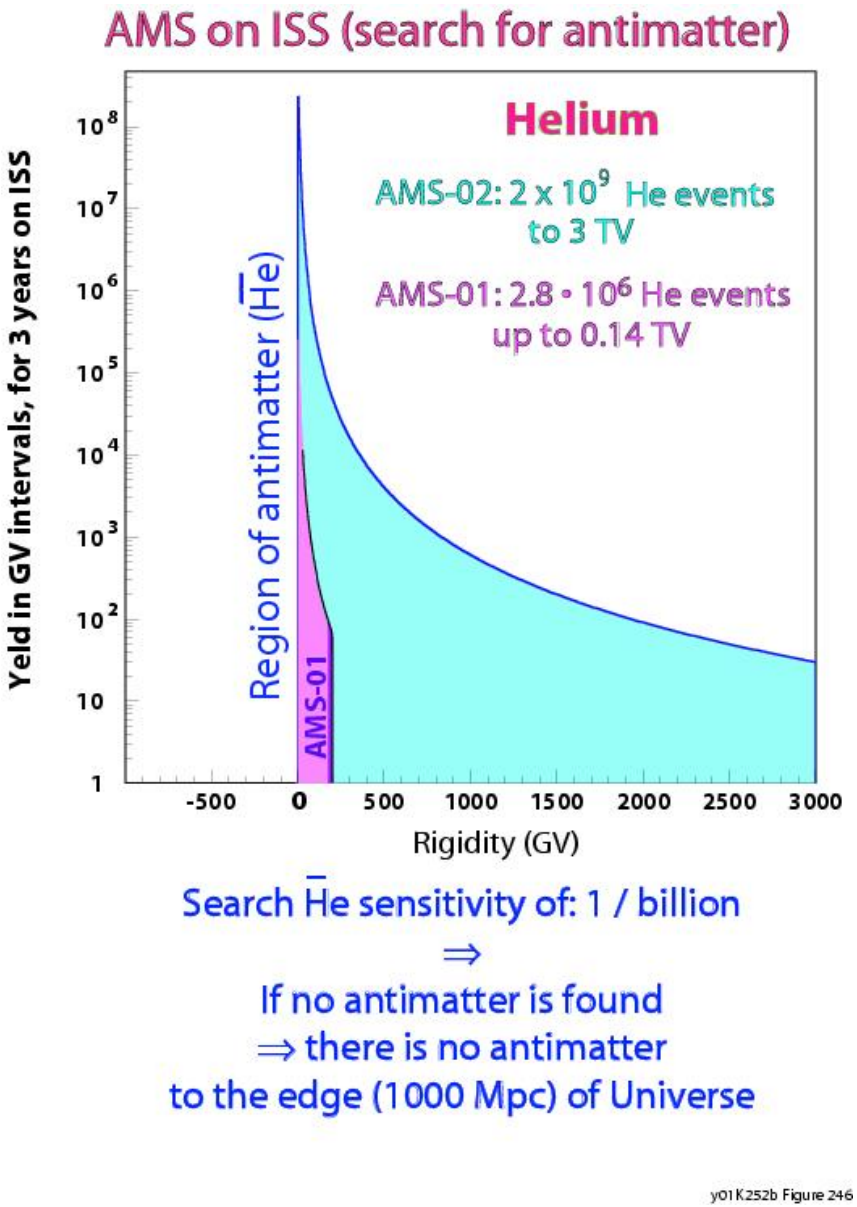

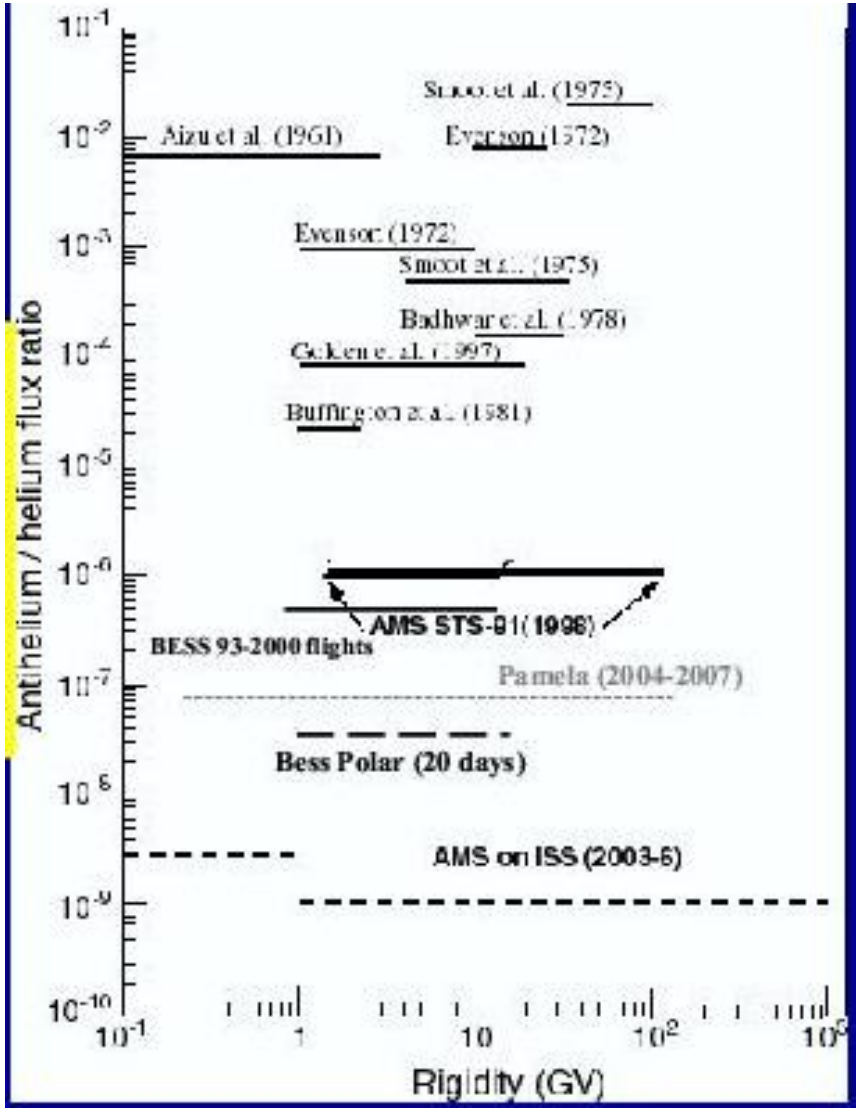

Conclusions

– An area of Astroparticules is booming
– A sophisticated and complete detector will be available over a long observation period.
– Balloon flights lasting one to few months will soon be possible
– Space-borne experiments with multiple capabilities will soon fly (PAMELA, AMS-02)
– The construction and commissioning of the detector are a first class technological challenge.
– AMS-02 will contribute to the observation of cosmic rays and photons in space, complementary both in time scale and energy range to other projects.
– A rich and diversified physics program will result